

[REDACTED]

[REDACTED]

[REDACTED]

[REDACTED]

[REDACTED]

[REDACTED]

[REDACTED]

[REDACTED]

[REDACTED]

[REDACTED]

[REDACTED]

[REDACTED]

[REDACTED]

[REDACTED]

[REDACTED]

[REDACTED]

[REDACTED]

[REDACTED]

[REDACTED]

[REDACTED]

[REDACTED]

[REDACTED]

[REDACTED]


[REDACTED]

[REDACTED]



Abstract

This thesis presents the development of MultiFab, a multi-material 3D printing architecture that is high-resolution, scalable, and low-cost. MultiFab enables the 3D printing of parts with materials that interact optically and mechanically. The hardware is low-cost since it is built almost exclusively from off-the-shelf components. The system uses commercial piezoelectric printheads that enable multi-material 3D printing with a resolution of at least 40 μm . This thesis presents the design and fabrication of MiniFab, a 3D printer that implements the MultiFab architecture, and its key subsystems, including novel material feeding and UV LED curing systems. Additionally, results show that the printer is capable of producing multi-material parts for a wide variety of applications.



Acknowledgements

[REDACTED]

[REDACTED]

[REDACTED]

[REDACTED]

[REDACTED]

[REDACTED]

[REDACTED]

[REDACTED]

[REDACTED]

[REDACTED]

[REDACTED]

Table of Contents

1	Introduction	11
1.1	Thesis Overview	12
2	Background	13
2.1	Multi-Material 3D Printers	14
2.1.1	State of the Art.....	14
2.1.2	MultiFab	16
3	MultiFab Overview.....	17
3.1	Design Goals.....	17
3.2	Positioning System	18
3.3	Electrical System	21
3.4	Material Feeding	22
4	Hardware Design.....	24
4.1	Material Feeding System	24
4.1.1	Problem Description	26
4.1.2	Design Criteria.....	28
4.2	Material Curing System.....	28
4.2.1	Problem Description	30
4.2.2	Design Criteria.....	30
5	Hardware Implementation	31
5.1	Material Feeding System	31
5.2	Material Curing System.....	34
5.3	MiniFab Printer	35
6	Printing Process.....	38
6.1	Principles.....	38
6.2	Material Feeding	42
6.3	Material Curing	42
6.4	Evaluation	43
6.4.1	Calibration Pattern.....	43
6.4.2	Print Imaging	44

7	Applications.....	45
7.1	Functionally Graded Materials.....	45
7.2	Optically Functional Printed Devices	46
7.2.1	Fiber Bundles.....	46
7.2.2	Microlens Arrays	49
7.2.3	Caustic Devices.....	51
7.3	Complex Metamaterials.....	52
7.3.1	Negative Poisson Ratio.....	53
7.4	Appearance	54
7.5	Printed Fabrics	56
7.6	Conductive Traces	57
7.7	Printing Over Existing Objects.....	59
8	Conclusion and Future Work	60
9	Bibliography	62

List of Figures

Figure 1. Layer approximation of the slicing process.....	13
Figure 2. Objet500 Connex3 and 3D Systems ProJet 5500x multi-material 3D printers.....	14
Figure 3. Diagram of the multi-material SLS process.	15
Figure 4. Highlight of MiniFab’s positioning system axes.....	20
Figure 5. Electrical system block diagram.....	21
Figure 6. Pressure Control System Diagram.....	25
Figure 7. Diagram of Relevant Physical Parameters in Pressure System.....	26
Figure 8. Pressure system valve controller.	32
Figure 9. Bottom of Epson printhead.	33
Figure 10. Simplified setup of the micro-valve driven pressure control system.	34
Figure 11. UV LED Curing Module.	35
Figure 12. MiniFab Multi-Material Fabrication Platform.....	36
Figure 13. System axes of MiniFab.	37
Figure 14. Fully encased MiniFab 3D printer.	37
Figure 15. Image of material droplets with the proper driving waveform (left) and a sub-optimal waveform (right) taken with the JetXpert high-speed camera system.	40
Figure 16. Computer interface for changing the printhead driving waveform.....	41
Figure 17. JetXpert benchtop setup.	41
Figure 18. 3D chart pattern for the evaluation of single material printing.	43
Figure 19. Micro-CT image of the calibration pattern.	44
Figure 20. A 3D printed FGM slab with a rigid, ABS-like material, RIG-3 and a flexible material, ELA-4.	45
Figure 21. Diagram of the typical structure of an optical fiber.	47
Figure 22. An optical fiber printed with the MultiFab platform.	48
Figure 23. Microlens array lit by a point light source.....	49
Figure 24. Microlens array lit by a computer screen.	50
Figure 25. Caustic device 3D printed with MultiFab.....	51
Figure 26. Microwave frequency metamaterial cloak by Schurig et al. (Schurig et al. 2009).	52
Figure 27. Two-material metamaterial with a negative Poisson ratio.	53
Figure 28. Multi-color textured model of MIT building 10.....	54
Figure 29. Multi-material 3D printed wheels.....	55

Figure 30. 3D printed picture with back texture for light effects.....	55
Figure 31. 3D printed thin polymer fabric with a 90° grid pattern.	56
Figure 32. Printed fabric sample.....	56
Figure 33. Printed PEDOT pattern on glass.....	58
Figure 34. Printed silver nanoparticle conductive traces.	58
Figure 35. Parallax privacy screen 3D printed on a cell-phone.	59

1 Introduction

Additive manufacturing, or 3D printing, enables the rapid manufacturing of parts with complex geometries. The ability to effortlessly design and manufacture parts with complex geometries has enabled a new range of applications that have been previously impossible or impractical. Typically, most 3D printers use one or two materials: a modeling material and a support material that facilitates the printing of objects with overhangs and other complex features. The finite number of materials limits the functional applications of the aforementioned 3D printers. There is currently an evolution in progress with the emergence of a new generation of 3D printers that can print with multiple materials in one print. This new generation of 3D printers is enabling a new range of functional applications that will further advance the impact of 3D printing in society and industry.

So far, there are few available additive manufacturing platforms that can support the use of multiple materials in one object. The available options are expensive and feature closed architectures that do not allow further development and experimentation. MultiFab is a scalable architecture that redefines multi-material fabrication. This thesis will focus on the development of the MultiFab architecture with emphasis on MiniFab, a hardware embodiment and proof-of-concept. At a high-level, the key features of MiniFab are:

- **Multi-Material:** MiniFab can print with up to 10 materials and the architecture is scalable to support a larger number of materials.
- **Low-Cost:** The printer uses a combination of off-the-shelf components with novel approaches that enable high-resolution, low-cost printing.
- **High-Resolution:** The printer has a resolution similar to, and in some cases exceeds, that of industrial ink-jet printers.
- **Scalable:** MultiFab is a scalable software and hardware architecture that easily adapts to a wide range of evolving applications.

This thesis will focus on the mechanical development of the MultiFab architecture and will describe MiniFab, the hardware embodiment, in detail. The thesis will also highlight

the capabilities and potential applications of the printer through a variety of printed examples.

To summarize, the central thesis of this work can be expressed in the following statement:

I demonstrate the design and fabrication of a low-cost and high-performance multi-material fabrication platform.

1.1 Thesis Overview

The thesis starts in Chapter 2 by providing background on the current state-of-the-art and a high-level description of the motivations of the project. Chapter 3 provides an overview of the MultiFab architecture and its main subsystems. Chapter 4 describes the main mechanical challenges undertaken by this thesis while Chapter 5 describes the hardware implementation of the solutions to these challenges. Chapter 6 explains MultiFab's printing process and its main challenges. Finally, Chapter 7 showcases a variety of applications and printed examples.

2 Background

Additive manufacturing, commonly known as “3D printing”, is the process of fabricating an object by successively fabricating material layers. *Subtractive manufacturing* can be defined as the opposite process: material is removed from a stock piece of material to produce a final shape. 3D printing was invented in 1984 when patent #US4665492 for a “*Computer automated manufacturing process and system*” was filed by William Masters [1]. Until recently, perhaps due to the ubiquity and low cost of computing, 3D printing was unpopular and reserved for sophisticated engineering and design projects. 3D printing has become affordable and accessible, and it is starting to gain mass market acceptance as a consumer product.

All 3D printers operate under the same fundamental process. First, a 3D model of the desired object is created using computer 3D modeling software. The model is then tessellated and sliced by the printer’s software. The parallel slices represent the cross-sections of the object. The thickness of the slices is dependent on the resolution capabilities of the printer. After the set of slices that approximate the object are found, the printer’s software determines the raster sequence to physically produce the layers.

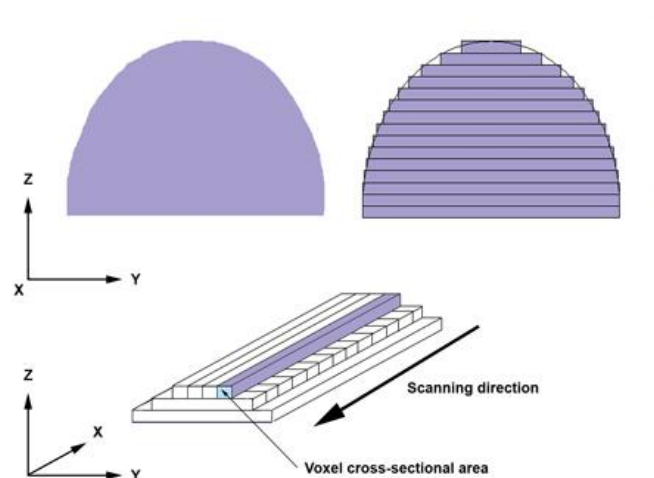


Figure 1. Layer approximation of the slicing process. The printer software determines the scanning sequence to fabricate the required layers. Source: Wikipedia

2.1 Multi-Material 3D Printers

Multi-material 3D printers are part of a new generation of 3D printers that can produce objects with two or more materials with spatially varying compositions. Multi-material fabrication has a myriad of yet unexplored applications that will inspire future research and stimulate a number of industrial markets.

2.1.1 State of the Art

There are currently two commercially available multi-material 3D printers: the Objet Connex series and the 3D Systems ProJet 5500x. These printers feature excellent print quality but their cost, typically in the \$250k range with materials priced at \$500 per kilogram, makes them inaccessible to most designers, researchers, and engineers. The material library is also limited and proprietary, supporting only UV-cured photopolymers. These printers can simultaneously use, at most, only three different materials. Finally, the hardware and software architectures for current multi-material 3D printers are proprietary and inextensible; changing the underlying software and hardware is virtually impossible.



Figure 2. Objet500 Connex3 and 3D Systems ProJet 5500x multi-material 3D printers. The Objet500 features three printheads and allows color printing. The price of these printers is in the \$300k range.

There have been significant efforts in the academic community to build multi-material fabrication platforms. Stereolithography (SLA) has been adapted to support multiple materials by using multiple vats with UV-curable polymers [2]; [3]; [4]; [5]; [6]. The systems provide high-resolution, but changing materials for each layer makes the printing process very slow. In addition, complex material gradients, necessary for many multi-material applications, are not supported by these systems. Several researchers have also experimented with using selective laser sintering (SLS) with multiple powders to obtain multi-material metal parts [7].

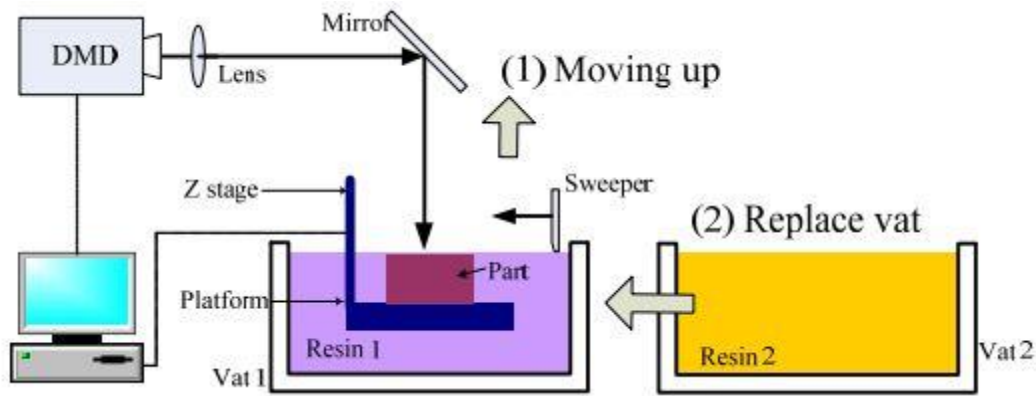


Figure 3. Diagram of the multi-material SLS process. Material vats are replaced for every layer that requires a different material. The process of changing the material vats is significantly slow and not easily scalable. Source: Zhou et al. (2013).

Multi-material inkjet-based systems have been developed mainly for tissue engineering applications and biopolymer printing [8]; [9]. The Fab@Home project has set a goal to develop an inexpensive, extensible, and multi-material fabrication platform. The current hardware supports printing with multiple syringe-based extruders and provides a library of materials [10]. However, Fab@Home's syringe-based extrusion achieves relatively low resolution.

Researchers have also developed a number of applications that take advantage of multi-material 3D printing. Processes have been built for the design and fabrication of: objects with desired deformation properties [11], objects with desired subsurface

scattering [12]; [13], lenticular prints [14], and actuated deformable characters [15]. Some recent applications include designing and printing co-continuous polymers [16], bio-inspired structures [17], printed optics [18], deformable soft robots [19], tough composites [20], and nanomaterial composites [21].

Recently, there has been progress in the development of multi-material 3D design. Vidimce et al. [22] propose a programmable pipeline and architecture for direct specification of multi-material objects. Chen et al. [23] describe a functional specification process that translates high-level specifications to multi-material 3D prints. The output of these processes can be used as an input to the MultiFab platform.

2.1.2 MultiFab

MultiFab is an ongoing, multi-disciplinary research project focused on developing a low-cost, high-resolution multi-material fabrication platform. The aim of the project is to provide a quality, accessible platform for researchers and hobbyists interested in developing a variety of functional multi-material applications. Within the MultiFab project, significant efforts have been undertaken to develop a scalable hardware platform and novel multi-material design tools.

Lan [24] described the mechanical development of OpenFab, the precursor to the MiniFab 3D printer that will be presented in this thesis. The work presented by Lan focuses on the development of the printer's positioning and support systems. Kwan [25] developed driver electronics for adapting off-the-shelf inkjet printheads for 3D printing. This thesis will mainly focus on the mechanisms necessary to enable the use of low-cost inkjet printing equipment for 3D printing and on showcasing potential applications of the platform.

3 MultiFab Overview

MultiFab is a multi-material fabrication platform. Multi-material fabrication presents specific challenges not found in single material fabrication systems. The main challenges are: printing support of a variety of material rheologies, technical complexity and cost scalability, chemical compatibility of printing materials, and high-resolution spatial deposition of the printing materials. This section will provide a high-level description of MultiFab's goals and the key subsystems that enable multi-material 3D printing within the required design constraints.

At its core, MultiFab is not a hardware platform, but a scalable architecture that can be embodied in a variety of hardware configurations. The scalability and flexibility of the architecture represents a breakthrough in low-cost multi-material 3D printing. MultiFab's novel architecture is an approach that breaks the design paradigms of incumbent multi-material 3D printing platforms— that high-cost equipment is required for high-resolution multi-material fabrication.

3.1 Design Goals

MultiFab's overarching goal is to develop a low-cost, multi-material 3D printing platform that is easily reconfigurable, in both hardware and software, for a variety of applications. It is intended to support novel research directions impossible with current multi-material printing platforms. The following list summarizes MultiFab's high level design goals which were the core principles behind all the hardware and software decisions.

- **Multi-material:** Multi-material capability is the key driver of novel 3D printing applications. The use of multiple materials enables novel applications by combining materials that interact mechanically and optically. This new design paradigm will require novel engineering and simulation methods.

- **Modular:** The modular nature of the platform allows the user to reconfigure the capabilities of the platform for a variety of evolving applications. MultiFab features a design that allows the user to add and remove modules as required by a specific application.
- **Low-Cost:** The relatively low-cost (BOM of about \$5,000) of MultiFab allows researchers from a diversity of areas to explore new applications with minimal economic risk to their research programs. Current multi-material platforms are cost-prohibitive for most researchers and provide little incentive and capability for hardware and materials experimentation and exploration.
- **High-Resolution:** MultiFab is high-resolution, sub 100 micron, for all materials. MultiFab's architecture allows users to 3D print objects at multiple scales: from hundreds of microns to tens of centimeters. The use of piezoelectric printheads also enables the micron-level mixing of materials. This capability opens new applications unachievable with 3D printers currently available in the market.

3.2 Positioning System

This section provides an overview of MultiFab's positioning system and its capabilities. The reader should reference Lan [24] for an extensive description of MultiFab's positioning and motion control system architecture.

Inkjet 3D printing requires the positioning of a printhead in three dimensions relative to a build platform: two planar dimensions are required to produce a single layer, and an additional dimension is required to reposition the system to fabricate successive layers. Generating three independent degrees of positioning movement requires a minimum of three independent degrees of actuation. Theoretically, this positioning may be carried out via a number of means, such as revolute positioning arms. In practice, a typical arrangement consists of three linear degrees of actuation corresponding to the linear X, Y, and Z axes of a traditional Cartesian coordinate system. While more exotic arrangements

may have specialized applications, three prismatic joints usually results in a simpler motion control problem.

At a high-level, MultiFab's positioning system features: three active and three passive degrees of freedom, a modular carriage, and an aluminum extrusion (80/20 Inc.) frame. The three active degrees of freedom will be defined as the system axes X, Y, and Z. The system axes (X, Y and Z) are arranged in a Cartesian prismatic arrangement for kinematic and fabrication simplicity. The current embodiment of the printer features three active (translations along global X, Y, and Z) and three passive (local platform rotation about X, Y, and vertical translation along the Z direction) degrees of freedom. The local platform Z axis is coupled to the global Z axis so we can say that the printer has 5 real degrees of freedom: global X, Y, platform-coupled Z, and local platform rotations about the X and Y axes. The passive platform rotation degrees of freedom are used to align the print substrate's plane with the positioning X and Y plane.

The X and Y axes are arranged in a series configuration to move the printer's carriage in a plane. In particular, the Y axis carries the X axis, which actuates the carriage. The X and Y axes are actuated by high-torque stepper motors. The three active degrees of freedom are provided by three 1.8° stepper motors (Automation Technology KL17H247-168-4B for the X and Z axes and KL17H247-168-4B for the Y axis) driven by 16 micro-step stepper drivers (Big Easy Driver ROB-11876). The X and Y axes are driven by a stepper-belt configuration and the Z axis is driven by a stepper-lead screw configuration. As described by Lan (2013), the stepper-belt configuration is appropriate for the fast movements required for printing in the X and Y axes while the stepper-lead screw configuration is appropriate for the small and infrequent movements required by the Z axis. Figure 4 shows MultiFab's system axes.

The system provides a positioning resolution of 11.7 x 11.7 x 1.3 microns (2000 X 2000 X 20,000 DPI) in X, Y and Z respectively, almost an order of magnitude smaller than the inkjet printing process resolution (about 50 microns). The accuracy and precision of the system has been verified through the use of the machine vision system.

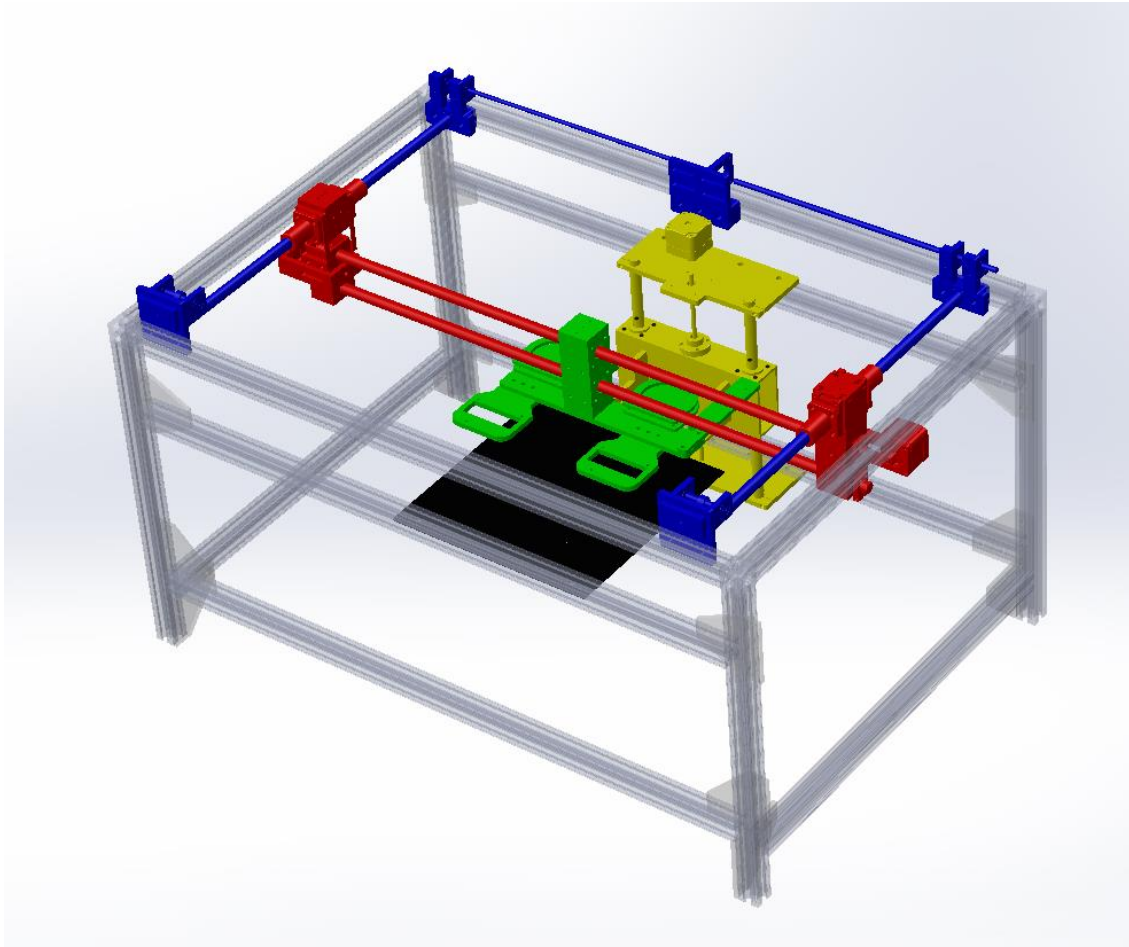


Figure 4. Highlight of MiniFab's positioning system axes. The X, Y, and Z axes are highlighted in red, blue, and yellow correspondingly. The carriage is highlighted in green. The build platform has three adjustment screws that allow the user to rotate the platform about the X and Y axes.

The positioning system drives a carriage that serves as a mount for the system's modules. The mounting system features a modular architecture that allows users to easily and quickly add, remove, and exchange modules. Subsequent sections will present the different modules that have been implemented in the current hardware embodiment of MultiFab.

3.3 Electrical System

MultiFab's entire hardware system is controlled by a central computer. The computer processes the layers of the 3D model and commands all subsystems in the printer. The central computer communicates with the subsystems via 100 Mb/s Ethernet and Universal Serial Bus (USB) protocols. Each subsystem has a dedicated microcontroller for local control. MultiFab's electrical system can be divided into the following subsystems: *positioning, printhead modules, UV-curing module, camera module, and material feeding*. The reader should reference Kwan [25] for a detailed description of MultiFab's electrical system. Figure 5 shows MultiFab's electrical system architecture.

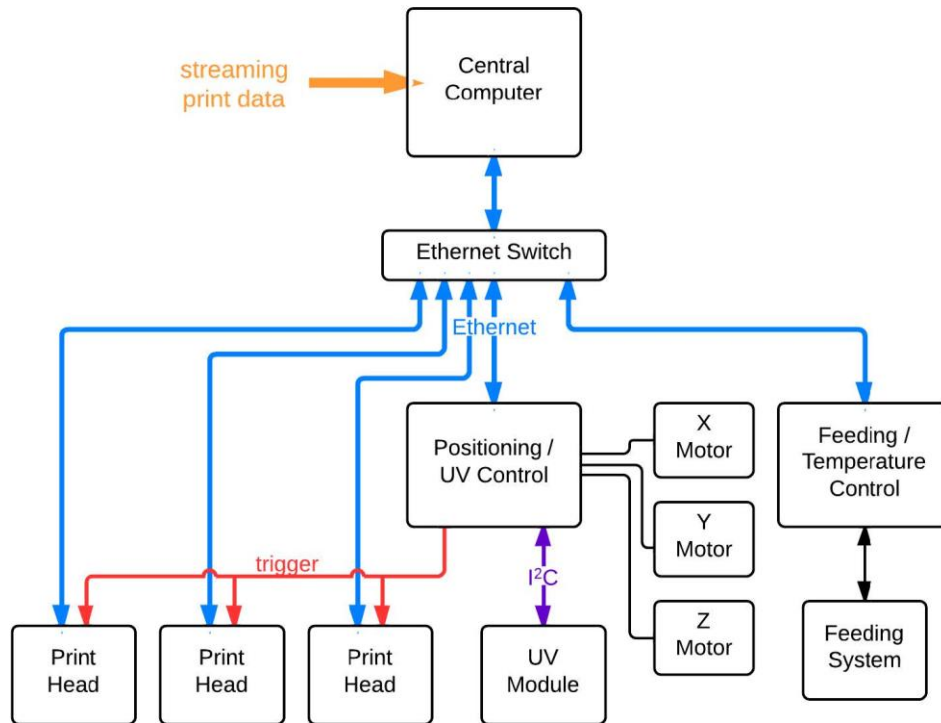


Figure 5. Electrical system block diagram. The electrical sub-systems connect to the central computer via Ethernet ports (blue connections). Image from [25].

MultiFab's architecture features a series of modules that are independent of the positioning system. Modules can be removed and added at the user's convenience for evolving applications and requirements.

MultiFab's main electrical subsystems include:

- **Positioning Subsystem:** Controls the position of the printheads relative to the build platform by actuating of the three stepper motors. The positioning subsystem translates commands from the central computer into directives for the motor drivers. It also senses the switching of the system limit switches during the axes homing procedure.
- **Printhead Modules:** Each module is comprised of an inkjet printhead and its drive electronics. The module receives print data from the central computer and it synchronizes printing with the positioning subsystem. As shown in Figure 5, the printhead drive electronics are triggered by the positioning commands.
- **UV-Curing Module:** The UV-curing module uses UV LEDs to cure materials deposited on the build platform by the piezoelectric printheads. It communicates with the central computer using USB protocol.
- **Material Feeding Subsystem:** The material feeding subsystem feeds printing materials –in the form of a jettable UV-photopolymer or a solvent-based liquid. The subsystem also maintains adequate pressure and temperature of the printing materials. The subsystem communicates with the computer using Ethernet protocol.

3.4 Material Feeding

The material feeding system is the critical subsystem that enables the use of commercial, off-the-shelf piezoelectric printheads. Commercial, off-the-shelf printheads have proprietary flow control systems compatible only with the printhead manufacturer's inks. These proprietary flow control systems do not support higher viscosity UV photopolymer materials needed for multi-material 3D printing. This problem is the main motivation for the design of a custom material feeding system capable of supporting

printing materials with a wide range of viscosities and surface tensions at room temperature.

The material feeding subsystem controls the flow of the printing materials from the material reservoirs to the printhead's nozzles. The key flow parameters that determine the jettability of the printing materials are: the liquid pressure at the inlet of the printhead and the material temperature at the printhead's nozzles. Monitoring and controlling the liquid pressure at the printhead inlet is not a static process due to hydrodynamic and hydrostatic pressure changes that occur within the flow control system. When the printhead is turned on, pressure changes occur in the time order of 1/10 seconds. This leads to the requirement of a fast and robust pressure control scheme as inappropriate pressure levels cause temporary malfunction of the printhead jetting.

In subsequent chapters, this thesis will explain the technical intricacies of material jetting. It is important to note that printheads can only jet printing materials that satisfy certain viscosity and surface tension constraints. These constraints are unique to each printhead's nozzle geometry. Printheads with similar nozzle geometries and piezoelectric actuation parameters will be able to jet printing materials within similar viscosity and surface tension ranges. Typically, the viscosity and surface tension of materials, particularly UV photopolymers inks, are not constant as they vary with temperature and fluid shear rate. The general heuristic is that viscosity decreases considerably with increasing temperature while surface tension decreases at a lower rate with increasing temperature. This heuristic led to a system that controls the temperature of the printhead's nozzles to maintain material viscosity and surface tension at the required range for proper jetting. As opposed to the pressure control of the printing materials, the control of the printhead's temperature is a more straightforward process since the heat transfer and dissipation processes are in the time order of 10 seconds.

4 Hardware Design

The hardware development process of MultiFab was driven by simple design principles and rapid hardware prototyping and testing. The design principles provided a foundation that constrained the design space, but still allowed ample experimentation and prototyping space. There is scant reference material on the design of inkjet-based 3D printing systems and most reference material is in the form of patents which provide few to no technical details for the reproduction of such systems. Guiding our design process with simple design principles and heuristics was critical to finding insights that led to a low-cost, but high-performance, hardware implementation. The following sections will focus on the design of the material feeding and material curing systems. The design of these systems is the focus of this thesis.

4.1 Material Feeding System

The material feeding system design was driven by the need to precisely and accurately control the pressure of the printing material at the inlet of the printheads. The piezoelectric inkjet printheads require precise and accurate control of their internal fluid pressure to properly operate. Fluctuations from the required nominal pressure can cause nozzle misfirings or inconsistent droplet size. Pressure fluctuations are caused by hydrostatic pressure changes due to material consumption during printing, and hydrodynamic pressure changes due to disturbances from printer movement and fluid flow pressure drops. To ensure that the fluid pressure at the inlet of the printhead is within the required threshold, a pressure control system was developed. The overall design requirements for the system are: scalability for multi-material and multi-printhead support, independent controllability of fluid pressure within ± 50 Pa, and compact and unobtrusive form factor.

In the current embodiment of the pressure control system, each printing material fluid is loaded in a 50 mL container. Material containers are placed on a rack mounted on

the printhead module and they can be independently interchanged for quickly adapting the printer to different printing applications. Alternatively, the material containers can be mounted outside the printer to support larger material volumes. Each container's internal air pressure is controlled by a micro two-way valve switching between 50 kPa and -3 kPa at 60 Hz. The fluid pressure is measured at the inlet of the printhead using a fluid pressure gauge. A proportional-integral-derivative (PID) feedback loop adjusts the switching period of the micro valve to compensate the pressure measured by the pressure sensor.

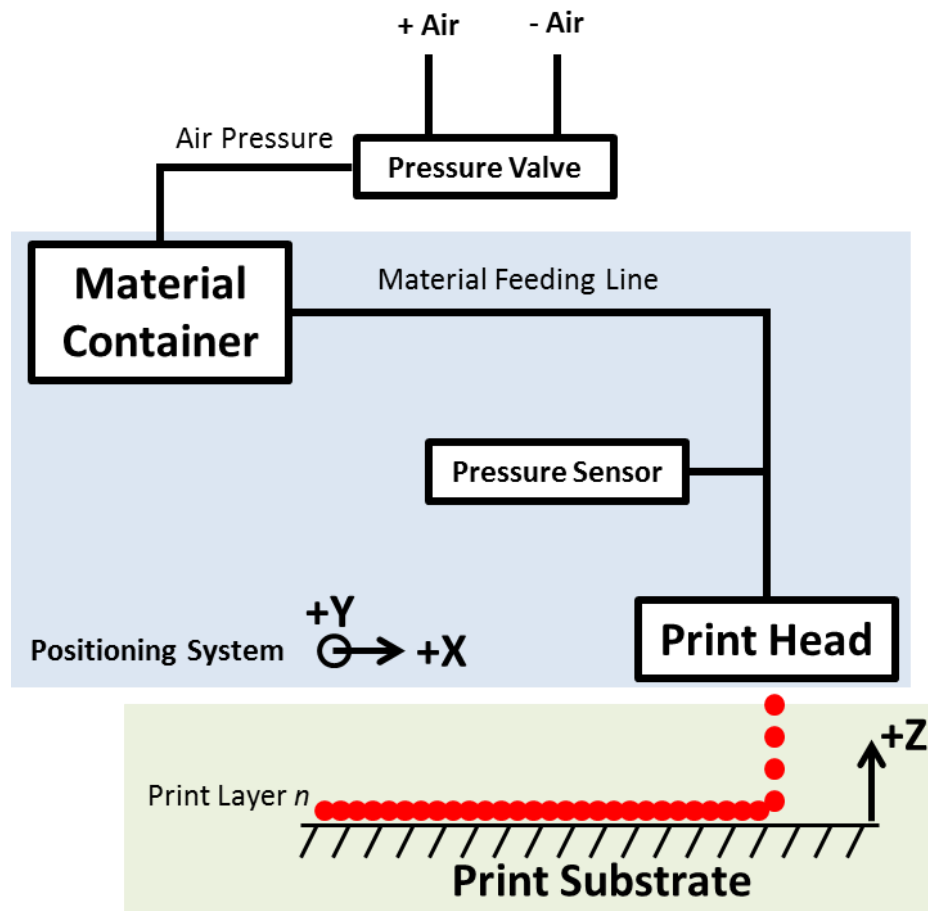


Figure 6. Pressure Control System Diagram. The part of the system that is mounted on the X and Y carriage is highlighted in blue. The Z axis platform, which serves as the print substrate, is highlighted in green. The micro valves control the air pressure in the material container which then feeds the material into the printhead at a set pressure. The material is jetted from the printhead onto the print substrate. Each material requires a micro valve, a material container and a pressure sensor. One printhead can hold up to 5 materials.

The micro valves for each material container are mounted on a compact manifold. The manifold is connected to common positive and negative pressure sources provided by two air pumps and appropriately damped and regulated. The use of a manifold and micro valve arrangement allows easy scalability for supporting additional materials.

4.1.1 Problem Description

At a fundamental level, the pressure control system's main function is to push material through a series of channels in a controlled and predictable manner. The main system control parameter is the pressure at the material inlet of the printhead. The system comprised by the material reservoir, the tubing, and the printhead internals poses a resistance to the flow of the printing material to the printhead nozzles. The complexity of the resistance of the system can be captured by a few design parameters. The flow resistance function is summarized in equation 1 below. Figure 7 depicts the physical representation of the parameters mentioned.

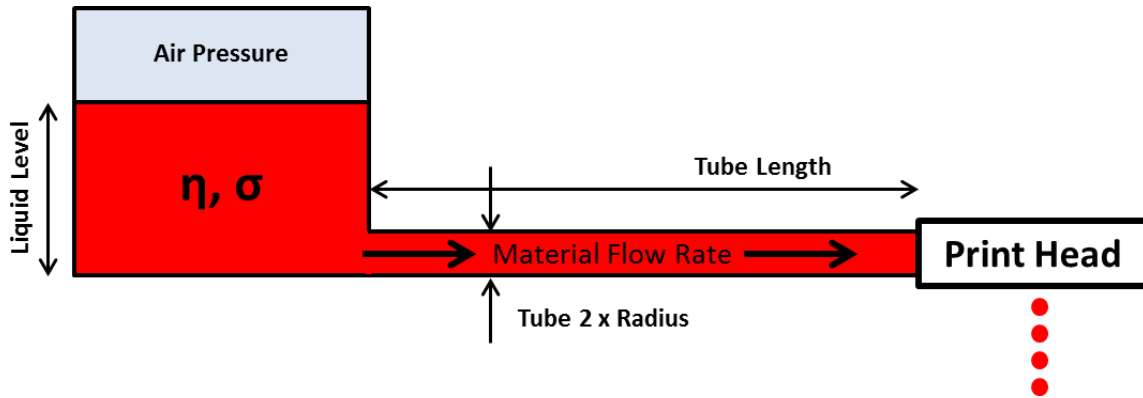


Figure 7. Diagram of Relevant Physical Parameters in Pressure System. The printing material (in fluid state) is highlighted in red. The air pressure in the material container is highlighted in blue. The material, with a viscosity σ and surface tension η , flows at a given flow rate from the material container to the printhead through a tube of radius R . The flow rate is determined by the size of the droplets printed and the firing frequency.

$$R(\text{Tube length and Radius, Material Flow Rate, Viscosity and Surface Tension}) \quad (1)$$

Liquid flowing through a resistance system needs a pressure differential to sustain a given flow rate. In our case, the maximum approximate flow rate of the printing material flow is known. This maximum flow rate serves as the upper limit in the design space.

$$\text{Flow Rate} = n * f * V_{\text{droplet}} \quad (2)$$

Equation 2 shows that the maximum flow rate for a given printhead channel is dependent on the number of nozzles being fired, n , the firing frequency, f , and the volume of the droplets, V . In theory, our printheads experience a maximum flow rate of about 0.025 mL/s with a maximum of 180 nozzles firing, a max firing frequency of about 5,000 Hz, and a maximum droplet volume of 26 pL.

Understanding the maximum flow rate of the system allows choosing an appropriate pressure source to adequately satisfy the flow rate requirements. The resistance R , of the system can be verified by a variety of experimental and theoretical schemes, but given the low speed of the flow (and thus a small Reynolds number, in the range of 100 for most of the printing materials used) in the tubing, the Hagen-Poiseuille equation (equation 3) provides a quick order-of-magnitude estimate of the required pressure to sustain a given flow rate.

$$\Phi = \frac{\pi R^4 |\Delta P|}{8 \eta L} \quad (3)$$

For the chosen tube diameter, $2R$, of 1/8 inches, a typical material viscosity, η in the order of 100 cP (at room temperature), and a maximum tube length, L , of 3 inches yields a required pressure differential of about 8 psi or 55 kPa. The total pressure at the material inlet is given by adding the pressure components from the hydrostatic pressure in the container and the internal air pressure in the container. The internal pressure in the container is the controlled parameter in the system.

$$\text{Pressure}_{\text{inlet}} = \text{Pressure}_{\text{hydrostatic}} + \text{Pressure}_{\text{container}} \quad (4)$$

$$\text{Pressure}_{\text{hydrostatic}} = \rho * g * h \quad (5)$$

The hydrostatic pressure is provided by the difference in height between the container liquid level and the printhead inlet. The typical container height difference, h , is about 8 cm. Typical material densities, ρ , range from 800 kg/m³ to 1500 kg/m³. This yields a typical hydrostatic pressure of about 800 Pa. This leads to the conclusion that the hydrostatic pressure, and the magnitude of its dynamic changes are much smaller than the pressure differential provided by the air in the container (equation 6), thus it can be ignored.

$$Pressure_{container} \gg Pressure_{hydrostatic} \quad (6)$$

The above exercise leads to the conclusion that the required pressure for full flow conditions (26 pL droplets, 180 nozzles, at 5 kHz firing frequency) is in the order of 8 psi. This estimate does not take into account several effects such as: the higher material temperatures near the material inlet which lower the liquid viscosity, the shear thinning effects typical of the rheology of UV photopolymers, among others.

4.1.2 Design Criteria

The findings of the previous section allow designing a system that satisfies the functional requirement set by equation 2. To satisfy the 0.025 mL/s flow rate criterion, the material feeding system has to provide a pressure of about 55 kPa (8 psi) in container pressure at maximum operating conditions with 1/8 inch tubing. This criterion guided the hardware selection process for the pressure control system.

4.2 Material Curing System

The UV-curing module is responsible for curing the photopolymer materials once they have been jetted out onto the printing substrate. Typically, industrial inkjet 3D printers use gas-discharge lamps to cure photopolymer materials. In this printer, UV LEDs are used to cure photopolymer materials with the purpose of lowering costs, facilitating

safe operation, and simplifying the light driving hardware. Compared to UV LEDs, gas-discharge lamps are conducive to more thorough curing due to their greater intensity and broader spectrum. Their high performance, however, is unnecessary for this printer, and therefore a compact, low-power, and low-cost curing system using UV LEDs was engineered to cure photopolymer materials. Gas-discharge lamps require high voltages (usually kilo volts) and currents which make them dangerous for desktop operation.

The fundamental description of light transmittance through a solid is given by the Beer-Lambert law. Photopolymers are subject to the Beer-Lambert law. It serves as a rule for the design and characterization of the UV curing process. The Beer-Lambert law is stated in equation 7. This derivation is given by Darsono et al. [26].

$$A = -\ln\left(\frac{i(x)}{I_s}\right) \quad (7)$$

The absorbance, A , is the amount of energy absorbed at a given depth, x . I_s describes the amount of light irradiated from the surface of the material. The intensity $i(x)$ is given by equation 8.

$$i(x) = \frac{I_s}{\exp\left(\frac{x}{D_p}\right)} \quad (8)$$

In equation 8, D_p is the depth at which the irradiance is $1/e$ times that of the surface. In addition, the curing of photopolymers requires a critical level of energy exposure. The critical level, E_c , describes the point at which the photopolymers turn from liquid to solid. The exposure of the polymer is given by $e(x,t) = i(x)t$. This leads us to a maximum curing depth of h from equations 9 and 10 where E_s is the exposure at the surface of the polymer.

$$e(x,t) = \frac{I_s t}{\exp\left(\frac{x}{D_p}\right)} \quad (9)$$

$$h = D_p \ln\left(\frac{E_s}{E_c}\right) \quad (10)$$

The above equations serve as a theoretical guideline to determine whether the UV light has sufficient power to cure a layer of thickness h .

4.2.1 Problem Description

Curing of the UV photopolymers used in MultiFab's printing process is an essential process that enables the formation of layered 3D structures. When material is deposited from the piezoelectric printheads onto the print substrate, it is in the form of a highly viscous fluid. The UV curing process provides the energy needed for the monomer units in the liquid photopolymer to properly polymerize to form a solid structure.

The process of converting the photopolymer from a liquid to a solid is a source of error. After the material is deposited on the printing layer and the UV light is shined on it, a chain reaction occurs. This might cause some uncured material to remain in the cured solid matrix. This causes shrinkage and curling on some materials and represents an important factor in the development and characterization of printing materials.

The main parameters of the UV curing system are the curing wavelength, the irradiance (power per unit area) of the UV source, and the radiant energy density (energy per unit area) at the printing layer. The light source has to be chosen so that it provides sufficient amount of energy at the curing wavelength. The curing wavelength is the wavelength at which the materials' photoinitiator starts the curing chain reaction.

4.2.2 Design Criteria

The UV LEDs have to satisfy the light intensity requirements of the material at the material photoinitiator wavelength. The UV LEDs have to be able to provide at least E_c at the curing depth h . Also, different materials, particularly those that have colored pigments, will exhibit varying levels of light energy irradiated at the surface, I_s .

5 Hardware Implementation

This chapter will describe the physical implementation of the two subsystems described in detail in Chapter 4. The two subsystems are part of the overall MultiFab architecture which integrates all subsystems into a working physical embodiment of the printer. This thesis will specifically discuss the implementation of MiniFab, a smaller, more compact, desktop version of the OpenFab 3D printer prototype presented by Lan [24].

5.1 Material Feeding System

The material feeding system is comprised of three main components: the pressure source, pressure sensing and control, and the container system. The system is built entirely from off-the-shelf, low-cost parts while still providing a ± 50 Pa precision pressure control for most materials. The hardware implementation was inspired by a previous design by McGuire et al. [27]. The design presented by McGuire et al. controls the pressure at the printhead inlet by controlling the air pressure in the material reservoir and maintaining a constant liquid level in the material reservoir. The design presented in this thesis controls the pressure at the printhead inlet by directly measuring the pressure at the inlet and controlling the air pressure in the material reservoir. The main advantage of the presented design relative to McGuire's design is that the system does not need to maintain a constant fluid level, significantly simplifying the overall design.

As described in Section 4.1, the material feeding system features a fast switching three-way valve per material channel to control the pressure value at the printhead inlet. In the current embodiment of the system, the three-way valves (LHDA1221111H, The Lee Company) are mounted on a modular manifold (LFMX0510538B, The Lee Company) that can accommodate up to 8 valves. Manifolds of different sizes and configurations can easily be fabricated for a variety of applications.

The Lee three-way valves were chosen for their small mass, fast-switching action (3-4 milliseconds), and compact form factor. The valves have a common, normally open, and normally closed port. The common port is connected to the material container. The normally open and normally closed ports are connected to negative and positive pressures respectively. The positive and negative pressures are provided by two pressure pumps (Airpon D2028 pumps). The outputs of the pumps are regulated by two miniature regulators (Airtrol 1/8 NPT R-800 and V-800 for positive and negative pressure respectively).

The three-way valves are driven by MOSFETs switching between +12 volts and +0 volts. The normal state of the valve (+0 volts) is a common channel connection to the negative pressure channel. The current embodiment of the circuit switches the valves at a frequency of 60 Hz. The circuit is simple, low-cost and low-power.

The MOSFETs are driven by a 16-channel I2C PWM driver board (Adafruit Industries 815). The PWM driver board also controls the actuation of the temperature control MOSFETs, which switch between +12 and +0 volts. The duty cycle of the PWM signal is controlled by a PID controller (Figure 8). The main disturbances in the material feeding system pressure are caused by: hydrostatic pressure changes due to material consumption during printing, hydrodynamic pressure changes due to disturbances from printer movement, and fluid flow pressure drops.

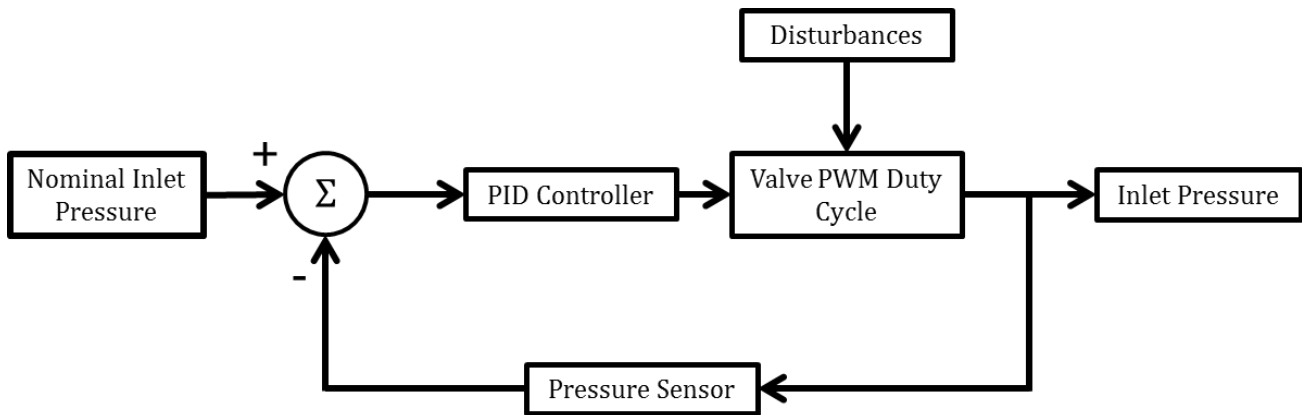


Figure 8. Pressure system valve controller. The PWM duty cycle of the valves controlling the pressure in the material reservoirs is controlled dynamically. The closed PID loop runs at 60 Hz which is sufficient to compensate for the changes and disturbances in the system pressure.

An accurate measurement of the inlet pressure is of utmost importance for the pressure control scheme to function properly. For this reason, a low mass, compact, fast pressure sensor was chosen. The barbed pressure sensor (Honeywell HSCD-LNN001PDAA3) is setup with a T-junction at the tip of each inlet. The sensor is fast (response time of 0.5 milliseconds) and accurate ($\pm 0.25\%$ Full Scale Span). The hermetic tubing (Norprene 1/8 inch) and a short air column between the pressure sensor sensing surface and the printing material ensures that the material in the tubing does not touch the surface of the sensor. This allows the user to use the same tubing and pressure sensor setup for other materials without having to change the setup.

Control of the printhead temperature is critical to maintain the printing material at the right viscosity for jetting. Control of the temperature is achieved with the same control scheme used for the pressure control valves. A +12 volt and +0 volt PID PWM control controls the current through two power resistors. The 5 ohm power resistors (Vishay TMC5-5.0-ND) are mounted on the stock metal grounding casing part of the Epson Workforce 30 printhead (Figure 9). The resistors are bonded to the stock metal casing using a one-part thermally conductive epoxy (Epoxy Set Inc., EB-403-1).

To measure the temperature at the printhead, an NTC thermistor is mounted on the printhead's metal casing. The sensor (Vishay NT-CALUG02A104H) is fast (1 second thermal time constant) relative to the thermal dissipation process (about 10 seconds). The PID controller controls the set point of the thermistor by controlling the current through the power resistors.

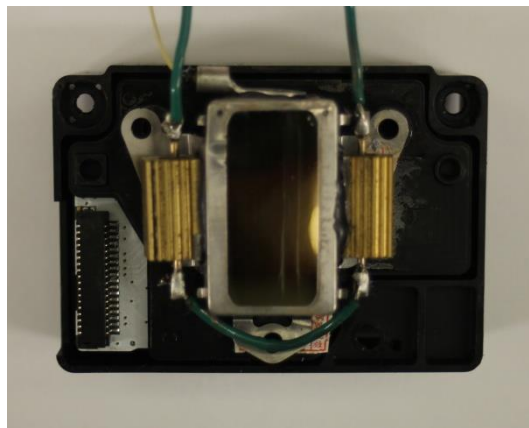


Figure 9. Bottom of Epson printhead. Power resistors (gold) are attached to the sides of the casing. The thermistor is visible at the top of the picture attached to the casing.

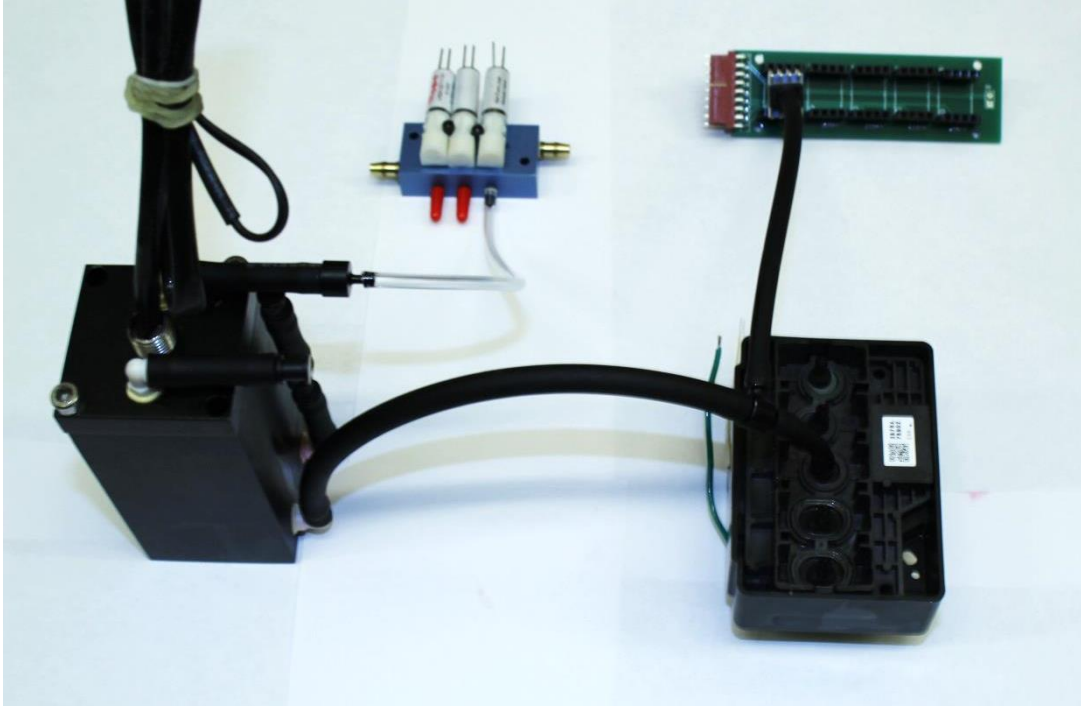


Figure 10. Simplified setup of the micro-valve driven pressure control system. The container (black) on the left holds the print material in liquid form. A valve connects to the material container to regulate its internal pressure. A pressure sensor monitors the pressure of the material at the inlet of the printhead in real-time. The valve switching is controlled by a PID controller that ensures consistent material pressures.

5.2 Material Curing System

The material curing system module consists of five UV LEDs (LEDEngin LZ1-00UV00) connected in a series configuration to a commercial LED driver (Recom RCD-48). The LEDEngin LEDs are currently the highest flux power 365 nanometer low-cost UV LEDs on the market. The LEDs also have a relatively flat efficiency vs. temperature curve which means that little efficiency (10% efficiency drop at 80°C relative to room temperature) is lost when the temperature of the LEDs increases. The LEDs are packed next to each other in a 3-2 configuration to ensure that their irradiance patterns overlap. This helps maintain a more uniform light intensity distribution over a larger area.

The module is fabricated out of aluminum and features a sliding mount to adjust the distance from the LED lights to the printing substrate. The module features a fan-cooled heat sink to ensure that the LEDs remain at low temperatures during operation.

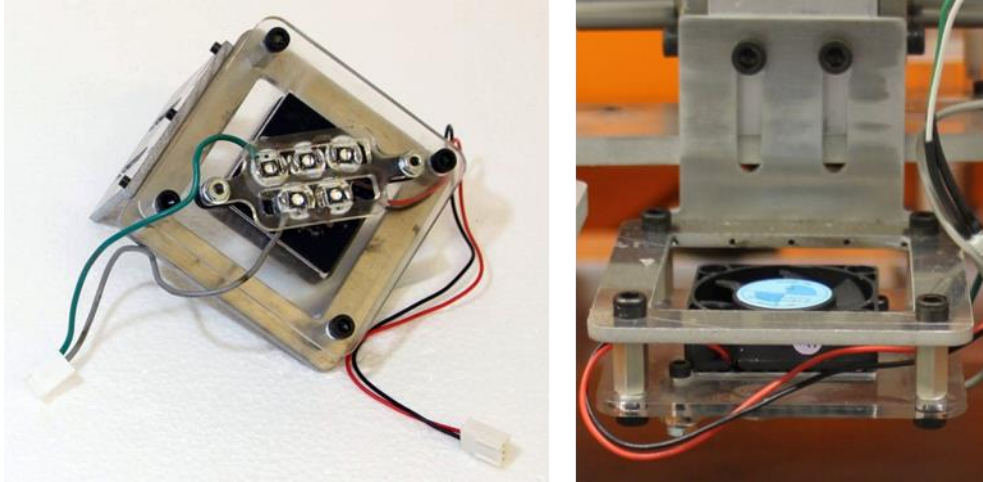


Figure 11. UV LED Curing Module. The LEDs are mounted in a 3-2 configuration on a compact fan-cooled heat sink. The heat sink ensures that enough heat is dissipated from the LED package to prevent significant efficiency loss. The right picture shows the attachment of the UV LED module to the positioning carriage. The distance from the LEDs to the printing substrate can be adjusted by changing the vertical position of the module.

5.3 MiniFab Printer

The MiniFab printer is a modified, desktop version of OpenFab. OpenFab is the precursor to MiniFab, presented by Lan [24]. MiniFab is the hardware embodiment of the MultiFab architecture presented in this thesis. The purpose of this improved prototype is to create a more robust, compact, and user-friendly version of the OpenFab printer.

MiniFab features two Epson Workforce 30 printheads, a single degree of freedom platform and an improved pressure control system. MiniFab's self-contained electronics box reduces overall system vibrations, increasing positioning, and printing accuracy and precision. The MiniFab printer is setting independent and can be operated wherever a 125 AC

outlet is available. The arrangement and packaging of the carriage assembly provide greater printing speeds, minimizing print times and decreasing the overall size of the printer.



Figure 12. MiniFab Multi-Material Fabrication Platform. The red box highlights the PC computer that controls the system. The blue box highlights the printing hardware, including the positioning system. The yellow box highlights the electronics box.

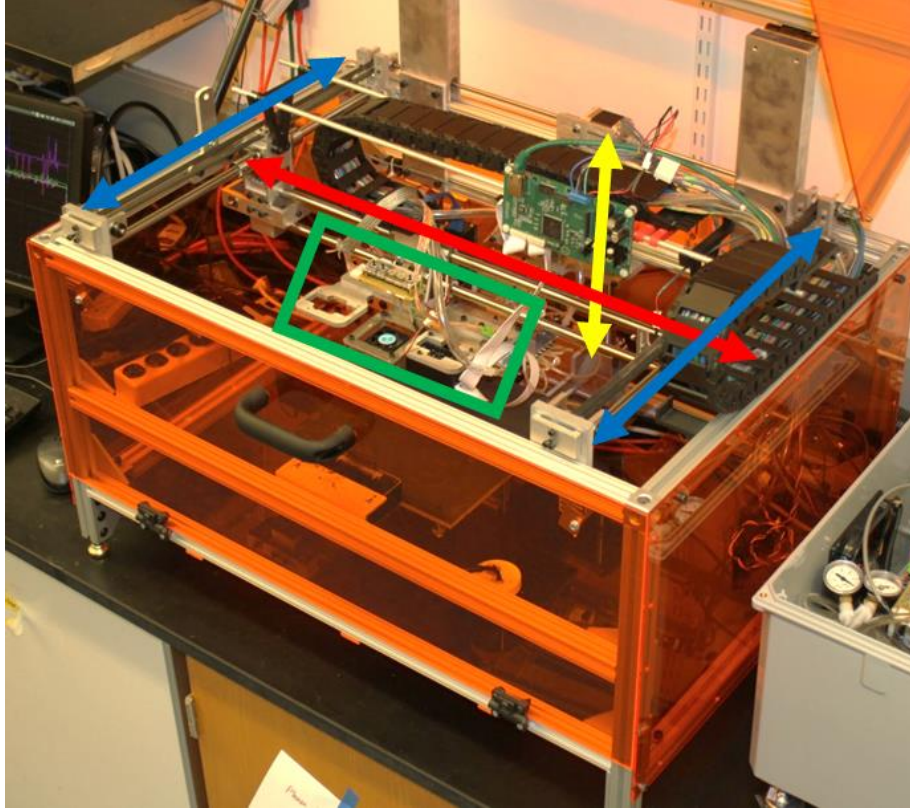


Figure 13. System axes of MiniFab. Blue, red, and yellow correspond to the Y, X, and Z axes of the printer. The printer carriage is highlighted in green.

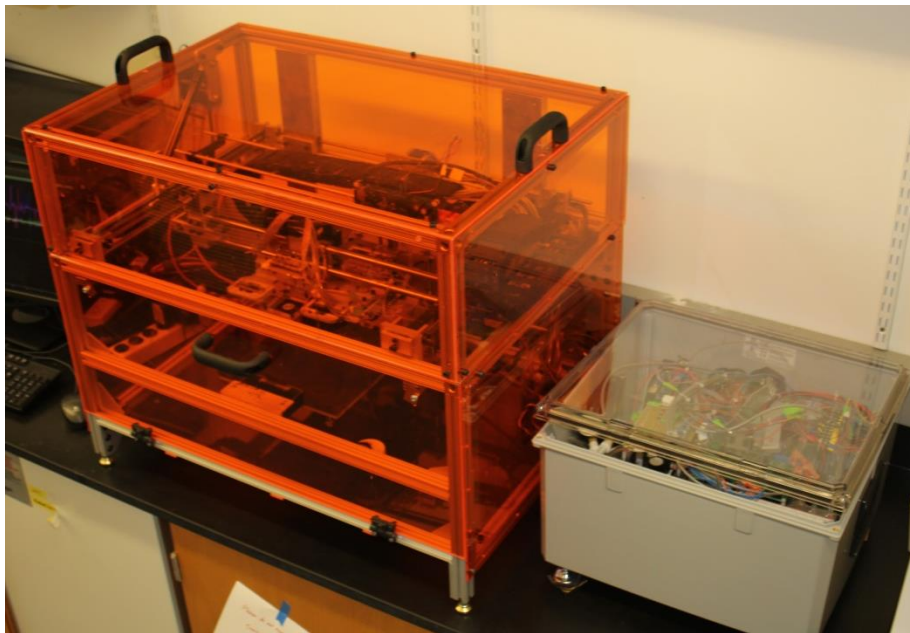


Figure 14. Fully encased MiniFab 3D printer. The cover protects users from the UV curing light.

6 Printing Process

This chapter will explain in detail the integration of all the different subsystems and components to build a multi-material printing platform. The printing process will be described.

6.1 Principles

Since MultiFab's focus is to enable a variety of applications, the useful material set must be as broad as possible. Material capabilities are primarily limited by the choice of printing technology, specifically the chosen printheads. The current embodiment of the MultiFab platform, MiniFab, employs Epson Workforce 30 printheads.

The MultiFab system uses piezoelectric inkjet technology as the core printing technology. Piezoelectric technology is particularly attractive because it is fast (6 kHz jetting frequency for off-the-shelf printheads), flexible (can accommodate a wide range of materials), high-resolution (40 micron resolution), and inexpensive (about \$75 per printhead). Piezoelectric inkjet technology does present some limitations which will be discussed in detail.

Piezoelectric inkjet printheads use piezo elements to create a pressure rise in a fluid chamber. The chamber has a nozzle exposed to ambient pressure conditions. When the piezo is actuated, the pressure rises in the chamber and material is pushed out of the chamber in the form of a stream or a droplet, depending on the actuation and fluid parameters. Printing materials have to satisfy the following constraints: adequate surface tension and viscosity, contain no particles larger than ~ 2 microns (or an order of magnitude less than the nozzle diameter), and has to be chemically compatible with the internals of the printhead and the pressure control system. The following list summarizes the material constraints; the high-level constraints listed guide the material design and selection process:

- **Static and Dynamic Fluid Properties:** The material has to satisfy a set of fluid properties for proper hydrodynamic behavior necessary for accurate and robust jetting from the printheads.
- **Chemical Compatibility:** The material must not interact negatively with the material feeding system and the internals of the printhead.
- **Curability:** The material must be curable with UV, thermal, chemical, or physical processes compatible with the inkjet process.
- **Physical Properties:** The material must be a liquid at jetting conditions and must have relatively low volatility at feeding conditions (pressures of about -400 Pa).

The most critical factors that have to be considered early in the material design process are viscosity and surface tension. These parameters can be used to estimate the jettability of the materials before they are even printed. Jettability refers to the propensity of a material to eject from a nozzle and form adequate spherical droplets adequate for printing. Low surface tension allows easy breakup of droplets into smaller droplets causing spraying. It also allows droplets to easily breakup when they impact the printing substrate, causing splashing. High surface tension limits the jettability of the droplets. On the other hand, high viscosity causes high flow resistance inside the printhead and low viscosity is usually preferable.

The physical parameters described can be summarized into a dimensionless number called the *Z number*. It is important to note that inkjet printing requires the atomization of the fluid jet. Continuous fluid jets do not allow precisely controlling the deposition of the printing materials on the two-dimensional, X and Y, printing plane.

$$Z = \frac{\eta}{\sqrt{\rho\sigma d}} = \frac{t_{visc}}{t_R} \quad (7)$$

In equation 7 above, η is the shear viscosity, σ is the surface tension, ρ is the density, and d is the jet diameter. McKinley et al. [28] provide an intuitive physical explanation of the *Z number*. They define the *Z number* as a ratio of the timescales of two different fluid processes: the Rayleigh inviscid fluid jet breakup, t_R and the viscocapillary dynamic

thinning of the viscous fluid, t_{visc} . Previous work has explored the jettability regime of the Z number. It is generally accepted to be in the order of $1 < Z < 10$ [29] or $4 < Z < 14$ [30].

Once the material has been engineered to satisfy the jetting constraints, the electrical signal that drives the piezoelectric elements in the printhead has to be optimized. Optimizing the electrical waveform allows controlling the velocity, size, and stability of the jetted droplets. A custom software and hardware platform for optimizing the printhead jetting was used to find the waveforms for various materials.

After the adequate waveform has been found for a given material, the material is tested in the printer by printing a calibration pattern. The calibration pattern allows the printer users to visually verify the printed properties of the material. It also serves as a design reference to evaluate the minimum sizes for a variety of common features. The calibration pattern will be discussed in further detail in section 6.4.1.

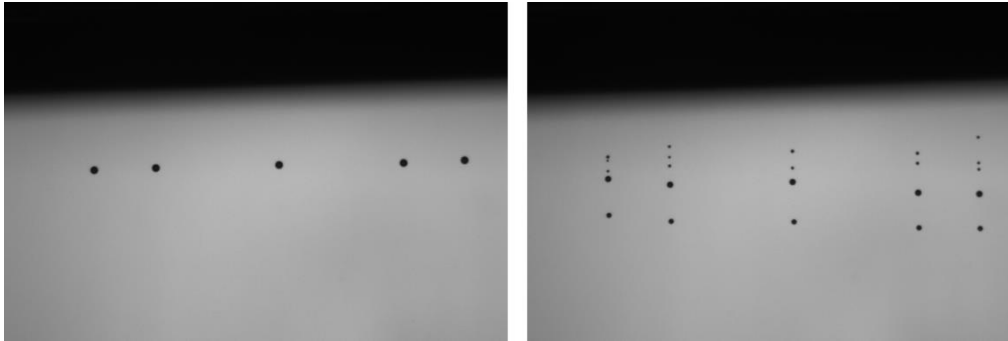


Figure 15. Image of material droplets with the proper driving waveform (left) and a sub-optimal waveform (right) taken with the JetXpert high-speed camera system. The droplets are about 30 microns in diameter. Undesirable satellite droplets can be clearly observed trailing the main droplet in the right image.

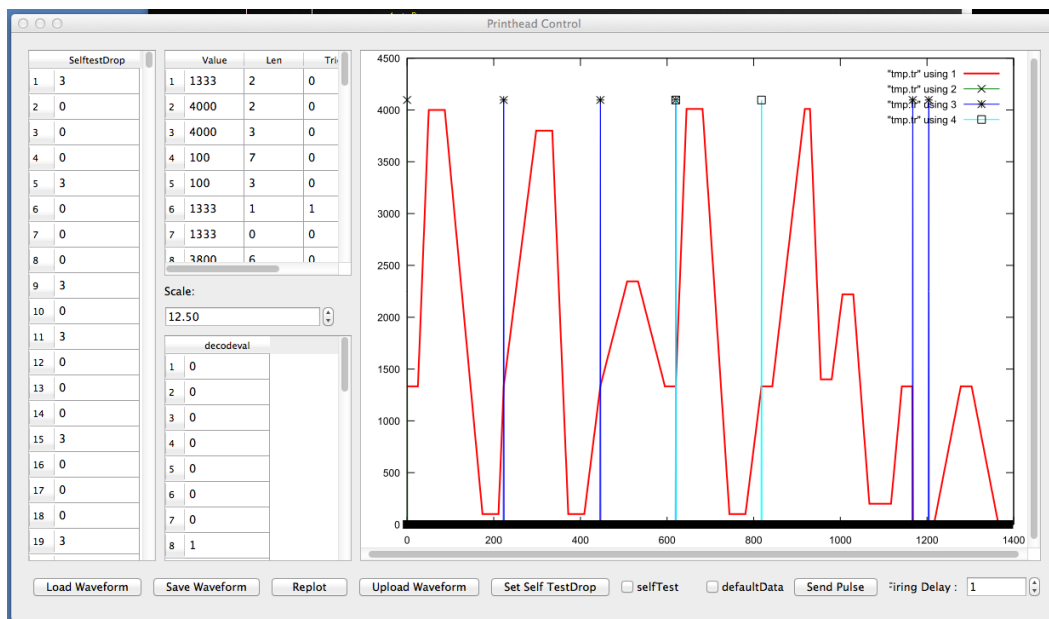


Figure 16. Computer interface for changing the printhead driving waveform.

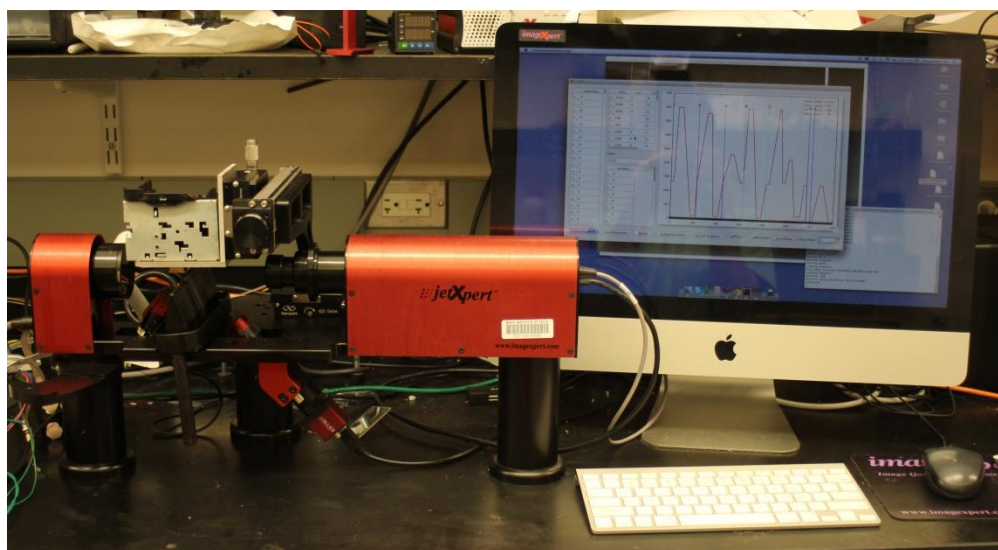


Figure 17. JetXpert benchtop setup. The JetXpert system allows to obtain real-time images of the jetted droplets. The computer provides an interface for controlling the printhead driving waveform in real-time. A waveform is found for each material using this system.

6.2 Material Feeding

The material feeding system is critical to the printing process; it controls in real-time the pressure of the printing fluids inside the printheads. Adequate pressure is required at all times for the printheads to operate properly. The material feeding system also controls the pressure during the printhead maintenance routines that happen at set time intervals during the printing process.

The first setup step before printing is loading the printing materials on the printhead. This is done by placing the material containers on the container rack and connecting the necessary tubing to the pressure control valves, the pressure sensor, and the printhead material inlets. When the tubing is initially connected, there are air pockets in the system. It is important to clear any air pockets from the tubing system to prevent nozzle misfirings. To clear air pockets, the printheads are moved to the cleaning station and the pressure is raised in the material tube that needs to be purged. The pressure is raised until printing material is observed flowing from the printhead face plate. After the material is purged, the positioning system automatically wipes the printhead on a rubber wiper that ensures that no material remains on the printhead face plate.

After the purging process is completed, the pressure is slowly reset to a nominal value of -400 Pa for printing. This pressure setting was found empirically and by referencing inkjet printing manuals [31].

6.3 Material Curing

The material curing process enables the solidification reaction in the photopolymers to create a solid 3D printed layer. After the material is deposited on the print surface, it starts to flow in a spreading mode. The time between the deposition of the layer and curing is critical to the topology of the final cured layer. Layers that are cured after a longer dwell time are usually smoother. However, long dwell times sacrifice high-frequency features and accurate reproduction of the input. Ideally, layers are cured immediately after the print

material is deposited to capture high-frequency features and faithfully reproduce the desired input.

6.4 Evaluation

After an object is 3D printed, it is useful to evaluate its quality relative to the desired input. There are several methods to determine the quality of the printed objects. This thesis will focus on two practical methods used throughout the course of the presented research: optical and volumetric inspection of a calibration pattern and direct print imaging of the object.

6.4.1 Calibration Pattern

A calibration pattern or 3D chart is useful for determining the printing capabilities of a 3D printer. Several calibration patterns were evaluated but most calibration patterns are intended for fused deposition modeling (FDM) printers. A custom pattern was developed. The pattern (Figure 18) contains several features for the evaluation of most print functions.

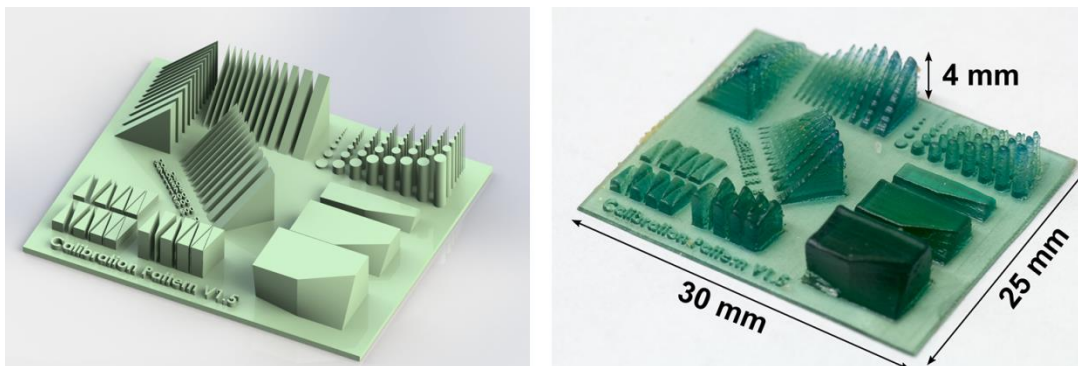


Figure 18. 3D chart pattern for the evaluation of single material printing. The left picture is a 3D rendering of the input 3D model. The right picture shows the printed chart.

The calibration pattern developed evaluates the following print features: maximum aspect ratio vs. feature size, minimum feature proximity vs. print height, maximum and minimum print angles, and maximum aspect ratio vs. feature height. These features provide sufficient evaluation basis for most 3D designs.

6.4.2 Print Imaging

An evaluation method explored is the 3D reconstruction of the printed 3D chart using micro computed-tomography (Micro-CT). Micro-CT is ideal for evaluating print quality because it can scan at multiple scales (millimeters to centimeters) with a resolution of about a micron. The method yielded good results; however, Micro-CT evaluation requires significant amount of preparation and handling time as compared to the desired iteration cycles.

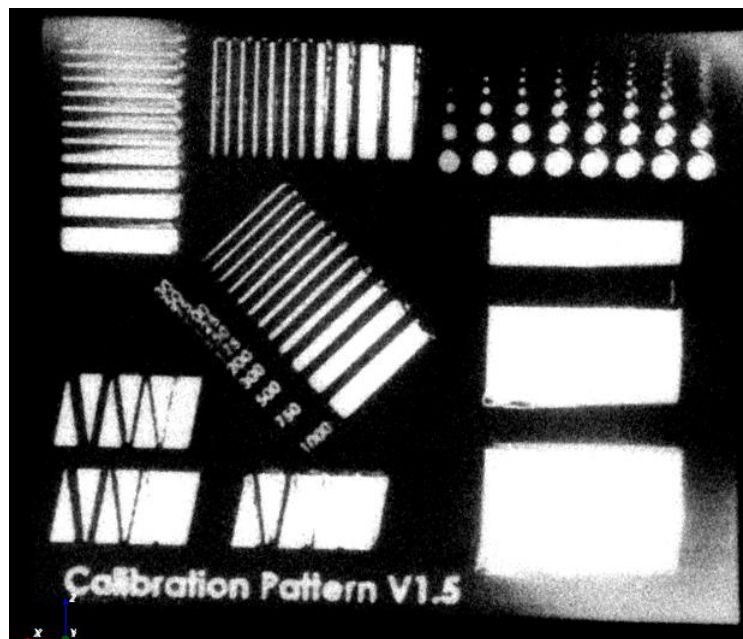


Figure 19. Micro-CT image of the calibration pattern. The image features some artifacts near the edges but can capture significant feature detail.

7 Applications

This chapter will present a wide variety of application examples and devices printed with the MultiFab architecture. The examples serve as proof-of-concepts for future development in the presented areas. The MultiFab platform is the first to enable the multi-material fabrication of a plethora of devices without major constraints.

7.1 Functionally Graded Materials

Functionally graded materials (FGM) enable the possibility of fabricating parts with varying spatial material distribution. The variation of the spatial composition of materials and their structure results in changes in the properties of the material. Previous work [7] in the area has focused on printing functionally graded metals. Little work has been done on printing polymer-based functionally graded materials [17]. This capability represents a monumental increase in the range of materials and properties that can be prototyped and fabricated.



Figure 20. A 3D printed FGM slab with a rigid, ABS-like material, RIG-3 and a flexible material, ELA-4. The materials are linearly graded from left to right: 0% RIG-3 and 100% ELA-4 in the left end to 100% RIG-3 and 0% ELA-4 in the right end. Note that the left end exhibits considerable flexibility relative to the right end.

7.2 Optically Functional Printed Devices

Optically Functional Printed Devices (OFPD) are 3D printed objects that interact with light sources to produce functional effects. The next sections present several OFPDs 3D printed with the MultiFab architecture. Previous work [18] has explored the functionality and practicality of OFPDs, concluding that useful functional devices can be printed.

The access to custom designed optical elements is severely limited. Prototyping an optical system is expensive and time consuming. The ability to 3D print and rapidly prototype embedded optical devices would be of great value to the engineering community. 3D printing is the intersection of optical, electro-mechanical, and functional fabrication.

7.2.1 Fiber Bundles

Optical fiber bundles are widely used in fiber-optic communications. They allow the transmission of light over long distances and at high bandwidths. Optical fibers are usually manufactured from silica due to its good optical transmission over a wide range of wavelengths. The fibers are made by a fairly complicated process that involves chemical vapor deposition to form a preform that is then pulled into a long and thin form. Although the process is suitable for mass-manufacturing, it does not have the flexibility to easily and quickly produce custom and complex fibers arrangements.

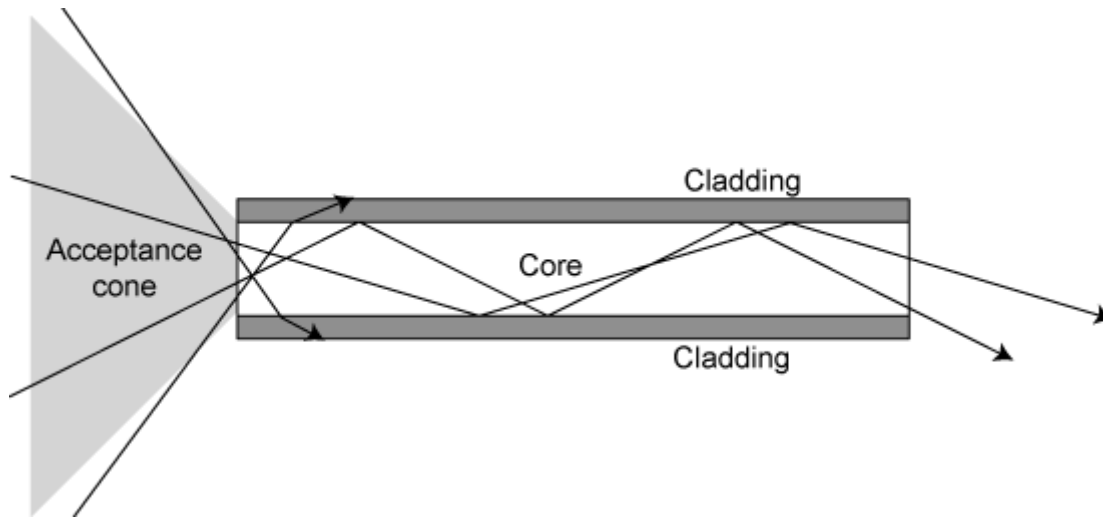


Figure 21. Diagram of the typical structure of an optical fiber. The transparent core is surrounded by a transparent cladding material with a lower index of refraction. The fiber acts as a waveguide due to total internal reflection. Source: Wikipedia.

An optical fiber with a 90-degree bend was designed with MultiFab's architecture by specifying a core with a high refractive material and a cladding with a low refractive index material. The materials, photopolymers HRI (High-Refractive Index) and LRI (Low-Refractive Index), were developed and serve as the core and cladding materials respectively. The fiber exhibited acceptable performance when tested with a 650 nanometer light source. Minimal light loss was observed and the fiber guided the light to a surface perpendicular to the light source orientation.

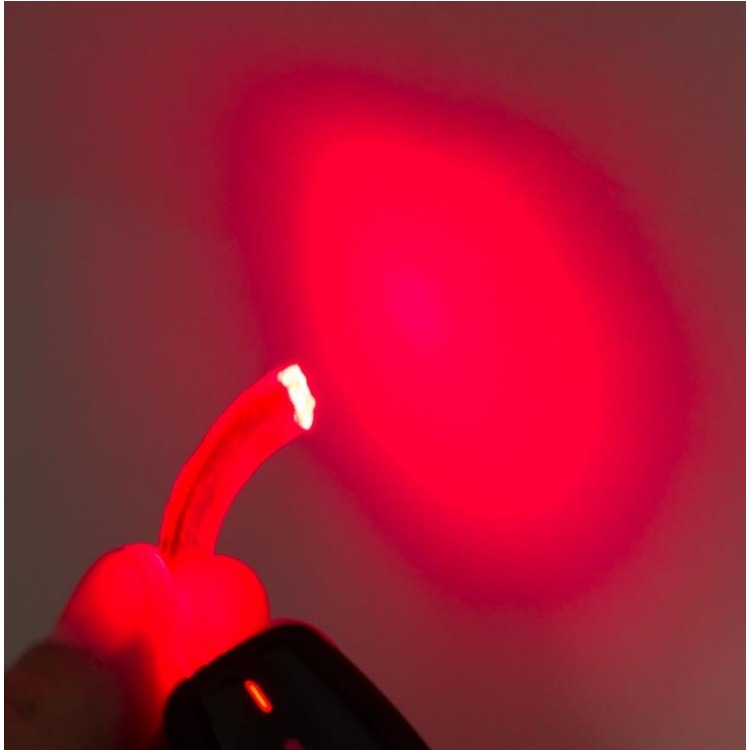


Figure 22. An optical fiber printed with the MultiFab platform. The fiber is shown guiding the light of a 650 nm laser pointer with minimal light loss. The core and the cladding of the fiber were fabricated with HRI and LRI respectively.

The optical fibers can be designed and fabricated into a variety of configurations for different applications. Previous work [18] has demonstrated possible useful applications of fiber optic bundles. The quick prototyping and fabrication of fiber optic bundles will enable a new range of applications that range from optical sensors to fiber bundle displays.

7.2.2 Microlens Arrays

The combination of custom optics with traditional display elements and in-the-loop-computation shows great promise as a way to build novel and better displays. Recent work in the field of computational displays has explored and demonstrated the capabilities of this approach. However, access to custom designed optical elements is severely limited due to the lack of flexibility of traditional optics manufacturing techniques. The techniques require complex processes and expensive equipment that is not easily reconfigurable.

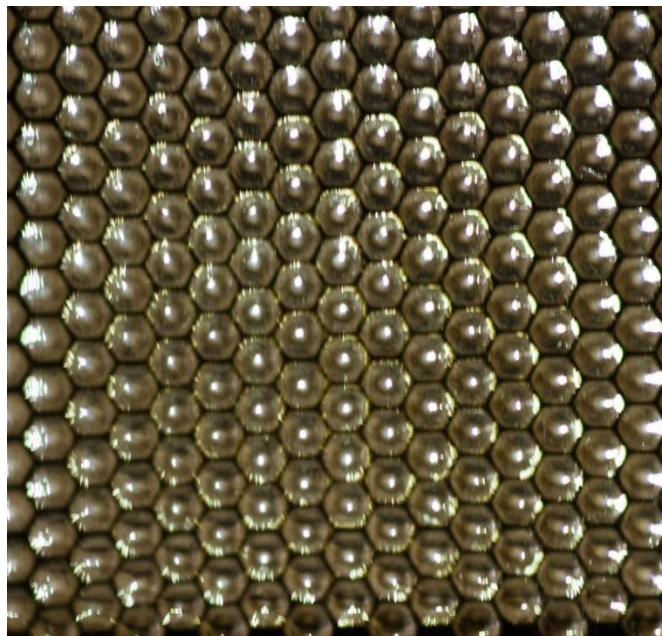


Figure 23. Microlens array lit by a point light source. Each lenslet has a size of 1 mm.

Figure 24 below shows that MultiFab is capable of 3D printing custom high-quality microlens arrays. The example below has custom baffles, printed using optically opaque black material, inserted in between the optically clear lenslets. The microlens array can be directly placed on high-resolution screens to obtain a dynamic light field display.

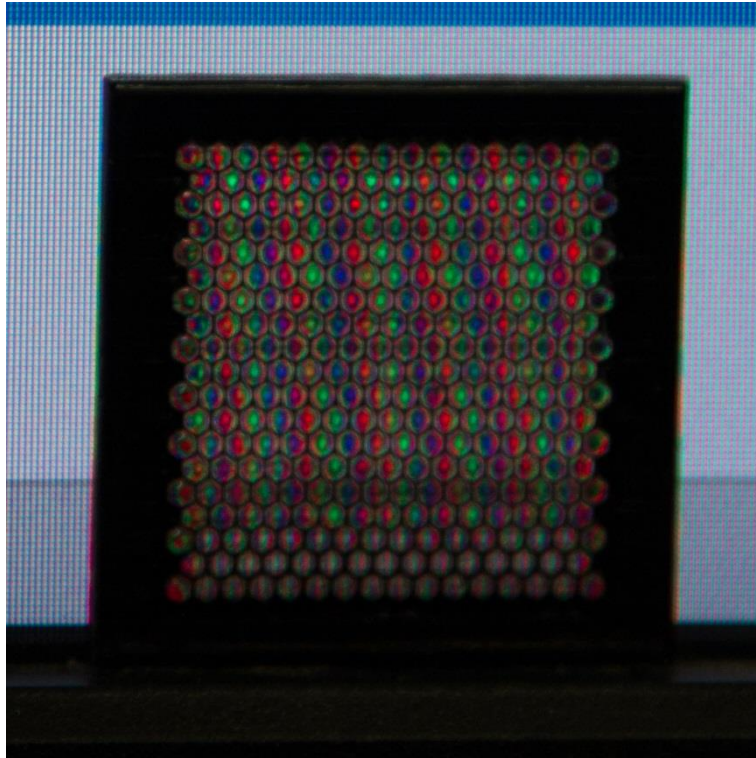


Figure 24. Microlens array lit by a computer screen. The lenslets reveal the Red-Green-Blue (RGB) pixels of the screen.

7.2.3 Caustic Devices

A caustic device is a transparent object with a refractive surface that redirects light from a source to form a desired image. Typically, the surfaces are machined using CNC milling. MultiFab enables the rapid 3D printing of high-quality custom refractive surfaces. The UV-curing process can be controlled to achieve the desired surface smoothness. In the case of caustic devices, the surface curing is delayed by a few seconds in order to produce a smooth surface. When the UV photopolymer is deposited on the last layer of the object it is allowed to flow for a few seconds before curing so it conforms to the previous layer.

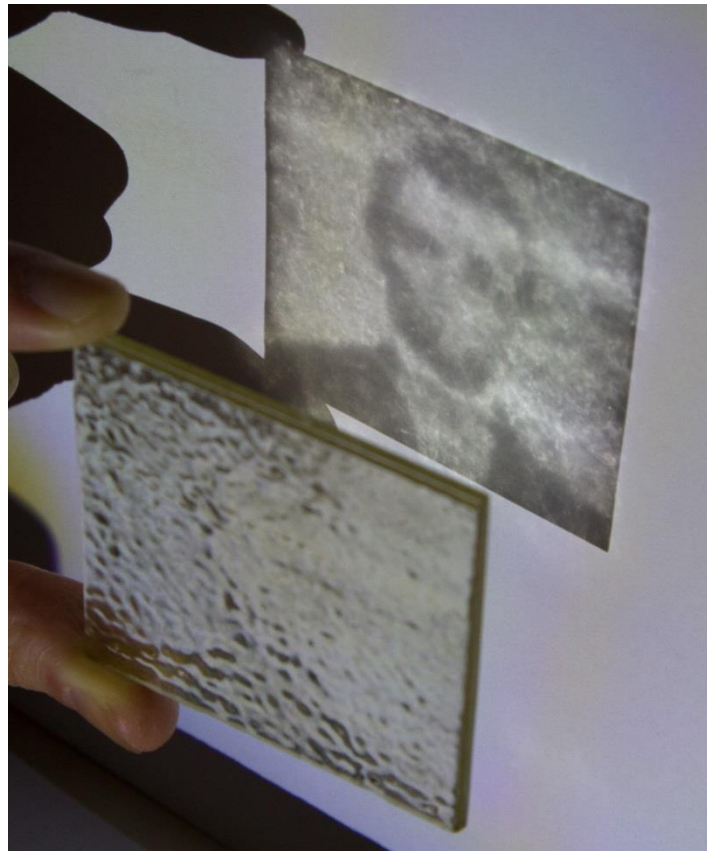


Figure 25. Caustic device 3D printed with MultiFab. The device is lighted from its anterior side and an image is projected onto the viewing plane. A white, point light source is used as the illumination source.

7.3 Complex Metamaterials

Metamaterials are an emerging class of materials that have engineered properties not found in its constitutive materials. Tailoring the shape, structure, geometry, and orientation of the constitutive materials can affect the optical, electromagnetic, acoustic, and mechanical properties of the metamaterial. Previous work has investigated the use of novel metamaterials for a variety of applications including: light and sound cloaking, negative and graded refractive-index, and negative Poisson ratio. The potential of combining multi-material fabrication and metamaterial structures is enormous.

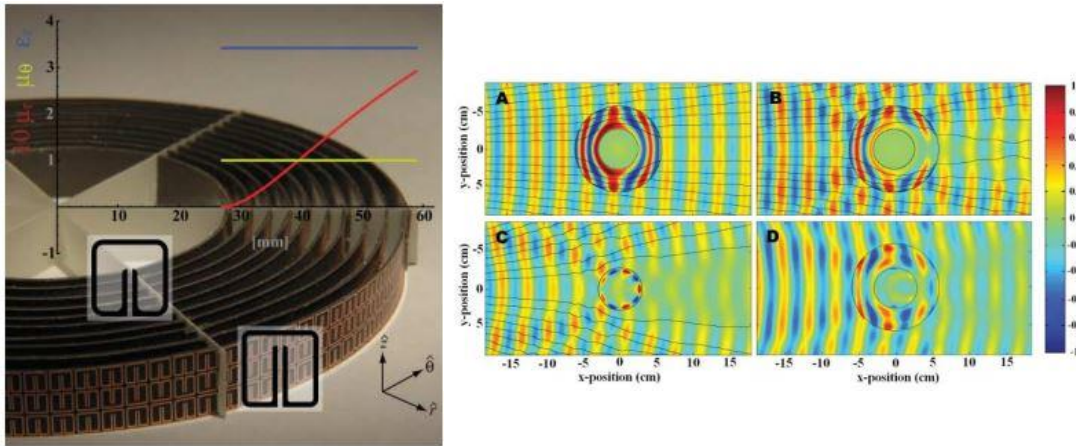


Figure 26. Microwave frequency metamaterial cloak by Schurig et al. (Schurig et al. 2009). The left image shows the internal structure of the copper metamaterial cloak. The right image shows the cloak made without metamaterial properties (C) and with metamaterial properties (D). A cloaking effect is achieved by designing a functional structure with copper, the metamaterial's constitutive material.

The MultiFab platform is capable of fabricating objects with a voxel resolution of about 40 μm . This enables designers using the MultiFab platform to design metamaterial structures with up to a 40 micron resolution. In practice, metamaterials with up to 10 constitutive materials can be fabricated using the MultiFab platform. Various metamaterial examples were reproduced using the MultiFab platform. This thesis will focus on the design of a two-material metamaterial with a negative Poisson ratio.

7.3.1 Negative Poisson Ratio

When forces are applied on materials they tend to expand or compress depending on the orientation and magnitude of the forces. Typically, materials tend to expand in the other two directions perpendicular to the direction of the force. This is called the Poisson effect. The Poisson ratio is the fraction of expansion divided by the fraction of compression. Equation 7 defines the Poisson ratio for the application being considered.

$$\nu = -\frac{\Delta W}{\Delta L} \quad (7)$$

In this application example the goal is to achieve a negative Poisson ratio by engineering the material structure. A hexagon structure with two materials was chosen. The two chosen materials are: ELA 4, a clear, flexible material, and RIG 3, a black, rigid material. The metamaterial achieved a slightly negative (0- ϵ) Poisson ratio.

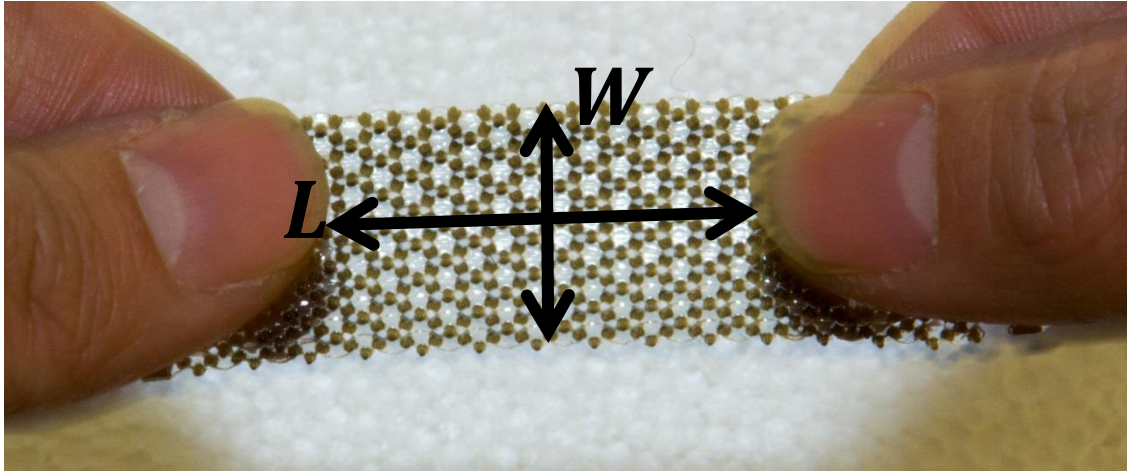


Figure 27. Two-material metamaterial with a negative Poisson ratio. When the material is pulled from its ends, its vertical width stays constant or expands slightly. This effect was achieved by designing and simulating the multi-material structure. In this example, two materials, ELA 4 (clear, flexible) and RIG 3 (black, ABS-like rigid), were used to create soft and rigid interfaces.

7.4 Appearance

The design and fabrication of objects that have appearance and texture properties is of interest for many applications. This capability allows designers to recreate color and texture properties quickly and inexpensively within a single design and fabrication framework (as opposed to having to use different fabrication processes and materials to recreate these properties).

In this example (Figure 28), the main building in MIT's campus was recreated with a checkered color and texture pattern. It contains three materials: RIG 3 red, RIG 3 black, and support, which fills a void in the interior of the building model. Materials were also developed to print color objects with the CMYKW color model.



Figure 28. Multi-color textured model of MIT building 10. The materials are RIG 3 red, RIG 3 black, and SUV (support). The texture was designed using the Foundry design platform. The object is about an inch cubed.



Figure 29. Multi-material 3D printed wheels. The left wheel contains five materials: RIG-3 black, red, and white, SUV 3, and ELA 4 clear. The right wheel contains two materials: RIG 3 black and ELA 4 white. The materials are graded from the outside wheel to the inside rim.

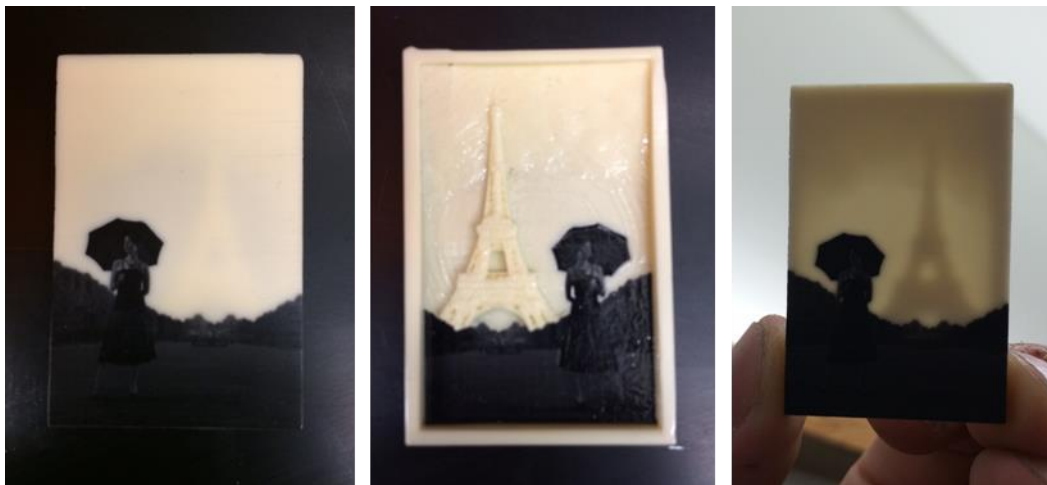


Figure 30. 3D printed picture with back texture for light effects. Two materials were used: RIG 3 black and white. The left picture shows the front of the 3D picture. The middle picture shows the backside with the raised detail. The right picture shows the results when the picture is exposed to backlighting.

7.5 Printed Fabrics

Printed fabrics are thin polymer membranes that have fabric-like textures and mechanical properties. The fabrics can be graded with both elastic and rigid materials, colored and arranged in a variety of configurations to obtain different patterns and properties. Support material can be deposited between the fabric fibers to ensure that they do not fuse together and to create link-chain structures. This method is flexible and more general than the traditional warp/weft patterns.



Figure 31. 3D printed thin polymer fabric with a 90° grid pattern. Colored symbols and letters were added to show the potential for fabricating elaborate patterns. The fabric is flexible and easily conforms to surfaces. The fabric is about 500 microns thick.

Printed fabrics could be used for appearance purposes: developing novel patterns and arrangements of fabrics. Also, if coupled with bio-compatible materials, printed fabrics could find their way in the manufacturing of custom scaffolds for wound repair or tissue engineering.

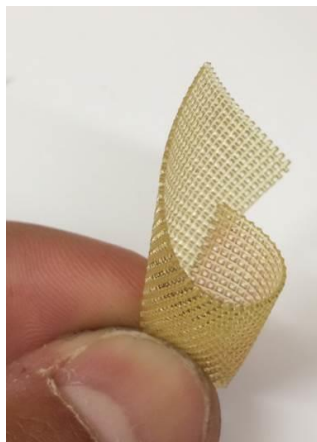


Figure 32. Printed fabric sample.

7.6 Conductive Traces

Embedding conductive traces in printed objects has been demonstrated to have enormous potential for enabling the freeform fabrication of functional devices and sensors. Conductive traces can serve as a medium for connecting embedded devices for a variety of applications that include sensing and kinematic applications. The work presented here is a preamble to a novel class of objects that will be able to sense and navigate an environment after being 3D printed.

There are two major approaches for embedding conductive traces in objects. The first approach is to suspend conductive nanoparticles in a solvent or any other jettable fluid that can be evaporated after printing. Once the particles are deposited on the substrate they are usually sintered using either high-powered lamps or heat. The second approach is to use a conductive polymer that is then dried to create a conductive film. The most commonly used conductive polymer is PEDOT:PSS or Poly(3,4-ethylenedioxythiophene). This thesis will present work on the development of the two approaches.

The printing of nanoparticles suspended in a solution presents several challenges. First, a solvent that has the right evaporation, rheology, and chemical compatibility with the suspended particles has to be chosen. Second, the conductive solution has to be kept at a negative pressure to satisfy the pressure requirement at the printhead channel inlet. Finally, the solvent has to be evaporated and the particles have to be sintered before subsequent layers of polymer can be printed.

After considerable experimentation, two compounds provided significant conductivity: PEDOT (Poly(3,4-ethylenedioxythiophene)-poly(styrenesulfonate), Sigma-Aldrich 739316) and a mixture of silver nanoparticles suspended in deionized water. The PEDOT can be directly printed and dried on the substrate. Typical resistivities for the PEDOT samples were in the order of 300 ohms/cm. The silver nanoparticle mixture does require sintering to achieve low resistivity. The particles were sintered in an oven for one hour at 100°C. Typical resistivities were in the order of 50 ohms/cm.

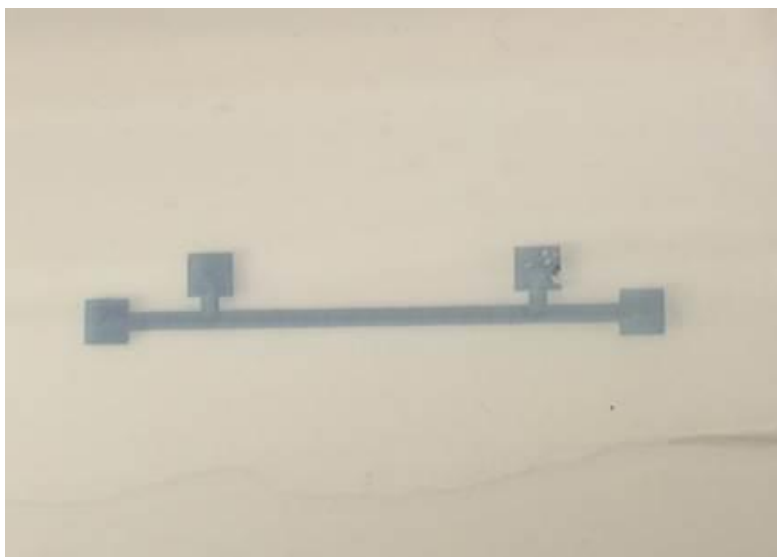


Figure 33. Printed PEDOT pattern on glass. The sample had a resistivity of about 300 ohms/cm. The PEDOT can be scratched off the substrate with ease.



Figure 34. Printed silver nanoparticle conductive traces. The traces have a resistivity of about 50 ohms/cm. The sample was sintered in an oven at a temperature of 100°C for one hour.

7.7 Printing Over Existing Objects

A novel capability provided by the MultiFab architecture and the MiniFab 3D printer is the 3D printing over existing objects. It is useful to support printing over existing parts and components. MultiFab features a print alignment procedure that allows accurate positioning of the 3D print with respect to the existing part. This capability could be used to enhance the functionality of existing objects by integrating optical or mechanical components. It could also be used as a customization tool to enhance the appearance or ergonomics of an object.

The print alignment is done via the integration of machine vision in two modes. The first mode is by capturing an image of the existing object on the print platform and then aligning the print with the object. The second mode is based on clicking a few corresponding points between the existing object and the print model and computing the optimal transformation matrix. The current system allows printing over a planar surface parallel to the X-Y plane.

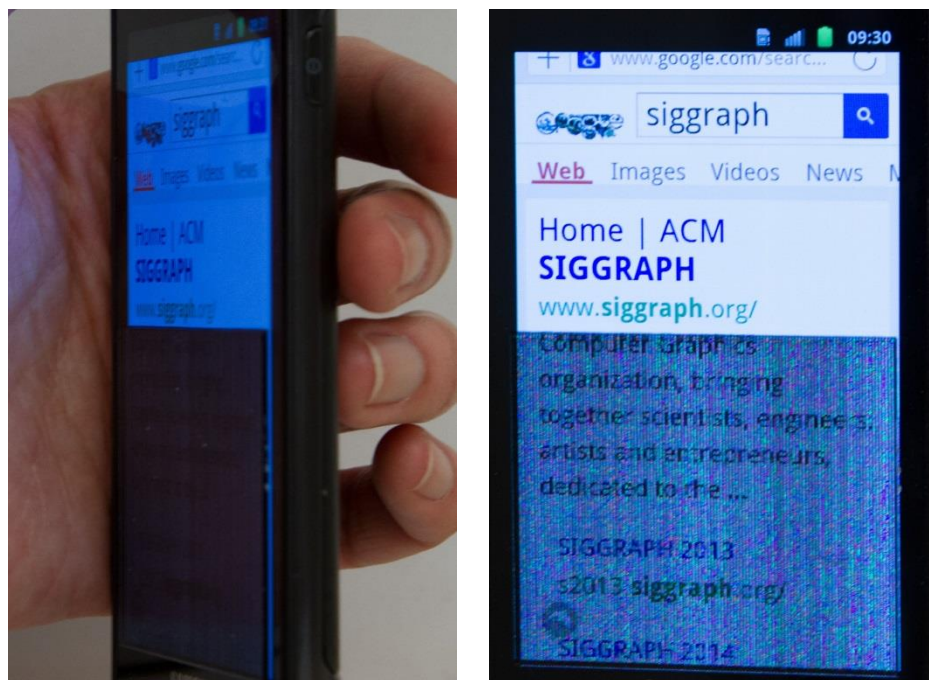


Figure 35. Parallax privacy screen 3D printed on a cell-phone. The privacy screen was printed with a clear material barrier with black vertical barriers that block the screen light when looked at an angle.

8 Conclusion and Future Work

This thesis presents the design and fabrication of a low-cost, multi-material, and high-resolution printer. Its focus is on two critical components necessary for enabling the use of off-the-shelf inkjet printheads: a novel micro-valve-driven material feeding system, and a UV LED light array for material curing. The use of off-the-shelf inkjet printheads for 3D printing is a novel approach that defies the current paradigm of multi-material printing—that high-cost equipment is necessary for high-resolution multi-material printing.

The pressure control system presented is low-cost, fast, and scalable to systems that require many materials. The system was designed, implemented, tested, and used for fabricating real functional multi-material objects. Additionally, a low-cost and scalable UV LED light array was developed. The UV LEDs represent a shift from gas-discharge lamps currently used in inkjet printing systems. The results demonstrate that the UV LED design is safer, simpler, lower cost, and powerful enough for multi-material fabrication.

The high-level design and hardware implementation of MiniFab was also presented. MiniFab is a low-cost (~\$5,000), desktop, multi-material fabrication platform. Results printed with MiniFab are comparable in quality to objects printed with high-end systems (>\$250,000). However, MiniFab offers a much wider range of material options not available in high-end systems. MiniFab, coupled with OpenFab, the multi-material design pipeline developed by Vidimce et. al. [22], represents a powerful disrupting combination that could enable a wave of novel applications for multi-material 3D printing. The possibilities with 3D printing are endless and this thesis presents a stepping stone towards the multi-material future that awaits us.

The research presented in this thesis is ongoing and focused on developing three key areas: novel materials, printing hardware, and real-time characterization of 3D prints. Also, further work will be done on the characterization of the curing process and on the chemical compatibility of multi-material mixtures. Further work on the hardware should focus on two areas: improving robustness of material feeding system and materials characterization.

The material feeding system could be simplified and other methods for measuring pressure in real-time should be explored. The materials, in combination with the UV LED modules, should be fully characterized for curing efficiency and chemical compatibility. The hardware is being continually improved and a future generation of the hardware will be geared towards providing 3D printing users with tools to fabricate novel devices that will disrupt the way design is currently practiced.

9 Bibliography

- [1] W. Masters, "Computer Automated Manufacturing Process and System". 2 July 1984.
- [2] S. Maruo, K. Ikuta and T. Ninagawa, "Multi-polymer microstereolithography for hybrid opto-MEMS," in *International Conference on Micro Electro Mechanical Systems*, 2001.
- [3] A. Inamdar, M. Magana, F. Medina, Y. Grajeda and R. Wicker, "Development of an automated multiple material stereolithography machine," in *Proceedings of 17th Annual Solid Freeform Fabrication Symposium*, Austin, Texas, 2006.
- [4] L. H. Han, S. Suri and C. E. Schmidt, "Fabrication of three-dimensional scaffolds for heterogenous tissue engineering," *Biomed Devices*, vol. 12, pp. 721-725, 2010.
- [5] J. W. Choi, H. C. Kim and R. Wicker, "Multi-material stereolithography," *Journal of Materials Processing Technology*, vol. 3, no. 211, pp. 318-328, 2011.
- [6] C. Zhou, Y. Chen, Z. Yang and B. Khoshnevis, "Digital material fabrication using mask-image-projection based stereolithography," *Rapid Prototyping Journal*, vol. 19, no. 3, pp. 153-165, 2013.
- [7] P. Kumar, J. K. Santosa, E. Beck and S. Das, "Direct-write deposition of fine powders through miniature hopper-nozzles for multi-material solid freeform fabrication," *Rapid Prototyping Journal*, vol. 1, no. 10, pp. 14-23, 2004.
- [8] S. Khalil, J. Nam and W. Sun, "Multi-nozzle deposition for construction of 3D biopolymer tissue scaffolds," *Rapid Prototyping Journal*, vol. 1, no. 11, pp. 9-17, 2005.
- [9] T. Burg, C. A. Cass, R. Groff, M. Pepper and K. J. Burg, "Building off-the-shelf tissue-engineered composites," *Phil. Trans. R. Soc. A*, pp. 1839-1862, 2010.
- [10] H. Lipson, D. Cohen, M. Heinz, M. Lobovsky, W. Parad, G. Bernstein, T. Li, J. Quartiere, K. Washington, A. Umaru, R. Masanoff, J. Granstein, J. Whitney and J. Lipton, "Fab@Home Model 2: Towards Ubiquitous Personal Fabrication Devices," in *Solid Freeform Fabrication Symposium*, 2009.
- [11] B. Bickel, M. Bacher, M. Otaduy, H. Lee, H. Pfister, M. Gross and W. Matusik, "Design and fabrication of materials with desired deformation behavior," in *ACM Trans. Graph.*, 2010.
- [12] Y. Dong, J. Wang, F. Pellacini, X. Tong and B. Guo, "Fabricating spatially-varying subsurface scattering," in *ACM Trans. Graph.*, 2010.
- [13] M. Hasan, M. Fuchs, W. Matusik, H. Pfister and S. Rusinkiewicz, "Physical Reproduction of

- materials with specified subsurface scattering," in *ACM Trans. Graph.*, 2010.
- [14] J. Tompkin, S. Heinze, J. Kautz and W. Matusik, "Content-adaptive lenticular prints," in *ACM Trans. Graph.*, 2013.
 - [15] M. Skouras, B. Thomaszewski, S. Coros, B. Bickel and M. Gross, "Computational design of actuated deformable characters," in *ACM Trans. Graph.*, 2013.
 - [16] L. Wang, J. Lau, E. Thomas and M. C. Boyce, "Co-continuous composite materials for stiffness, strength, and energy dissipation," *Advanced Materials*, vol. 23, no. 13, pp. 1524-1529, 2011.
 - [17] N. Oxman, "Variable property rapid prototyping," *Journal of Visual and Physical Prototyping*, vol. 1, no. 6, pp. 3-31, 2011.
 - [18] K. Willis, E. Brockmeyer, S. Hudson and I. Poupyrev, "Printed optics: 3D printing of embedded optical elements for interactive devices," *UIST*, 2012.
 - [19] J. Hiller and H. Lipson, "Automatic design and manufacture of soft robotics," *IEEE Transactions on Robotics*, vol. 29, no. 4, pp. 1-10, 2012.
 - [20] L. Dimas, G. Bratzel, I. Eylon and M. Buehler, "Tough composites inspired by mineralized natural materials: Computation, 3D printing, and testing," *Advanced Functional Materials*, vol. 23, no. 36, pp. 4629-4638, 2013.
 - [21] T. Campbell and O. Ivanova, "3D printing of multifunctional nanocomposites," *Nano Today*, vol. 8, no. 2, pp. 119-120, 2013.
 - [22] K. Vidimce, S. Wang, J. Ragan-Kelley and W. Matusik, "OpenFab: A programmable pipeline for multi-material fabrication," *ACM Trans. Graph.*, 2013.
 - [23] D. Chen, D. Levin, P. Didyk, P. Sitthi-Amorn and W. Matusik, "Spec2Fab: A reducer-tuner model for translating specifications to 3D prints," *ACM Trans. Graph.*, 2013.
 - [24] J. Lan, *Design and Fabrication of a Modular Multi-Material 3D Printer*, Cambridge, MA: Massachusetts Institute of Technology, 2013.
 - [25] J. G. Kwan, *Design of Electronics for a High-Resolution, Multi-Material, and Modular 3D Printer*, Cambridge, Massachusetts: Massachusetts Institute of Technology, 2013.
 - [26] N. Darsono, M. Hiroshi and O. Hiromichi, "Rheological study of the solidification of photopolymer and dispersed nanotube systems," *Applied Rheology*, vol. 21, no. 6, pp. 1-15, 2011.
 - [27] S. McGuire, C. Fisher, M. Holl and D. Meldrum, "A novel pressure-driven piezodispenser for

- nanoliter volumes," *Review of Scientific Instruments*, vol. 79, 2008.
- [28] G. McKinley and M. Renardy, "Wolfgang von Ohnesorge," *MIT Open Access Articles*, 2011.
- [29] N. Reis and B. Derby, "Inkjet deposition of ceramic suspensions: modelling and experiments of droplet formation," in *Materials Research Society Symposium Proceedings*, 2000.
- [30] D. Jang, D. Kim and J. Moon, "Influence of fluid-physical properties on inkjet printability," *Langmuir*, vol. 25, pp. 2629-2635, 2009.
- [31] Epson, "Service Manual: EPSON Stylus C110/C120/D120," [Online].